Polyoxometalates as nanoscale building blocks for the formation of functional materials

Zhang, Li Zhi

2009

Zhang, L. Z. (2009). Polyoxometalates as nanoscale building blocks for the formation of functional materials. Master’ s thesis, Nanyang Technological University, Singapore.

https://hdl.handle.net/10356/19310

https://doi.org/10.32657/10356/19310

NANYANG TECHNOLOGICAL UNIVERSITY

POLYOXOMETALATES MATERIALS

POLYOXOMETALATES AS NANOSCALE BUILDING BLOCKS FOR THE FORMATION OF FUNCTIONAL MATERIALS

ZHANG LI-ZHI

ZHANG LI-ZHI

SCHOOL OF MATERIALS SCIENCE AND ENGINEERING

2009

2009

POLYOXOMETALATES AS NANOSCALE BUILDING BLOCKS FOR THE FORMATION OF FUNCTIONAL MATERIALS

ZHANG LI-ZHI

School of Materials Science and Engineering

A thesis submitted to the Nanyang Technological University
in partial fulfillment of the requirement for the degree of
Master of Engineering

2009

Acknowledgments

I would like to express my sincere thanks to my supervisor, Assistant Professor Dong Zhili, for the constant encouragement and invaluable advice support that he has continuously provided throughout this work.

I would like to thank Professor Liu Xin in Nankai University for her constant supportive guidance throughout this research.

I would also like to make a grateful acknowledgement for Nanyang Technological University for providing the financial assistance.

Table of contents

Abstract

Polyoxometalates (POMs) are nano-sized metal-oxygen cluster species with a diverse compositional range and an enormous structural variety. They are powerful building blocks in the field of materials because of the following: (1) POMs can easily dissolve in water or organic solvent and hold the same polyoxoanion structure as that in the solid state; (2) POMs possess various charge, shape and bulk; (3) POMs can accept various numbers of electrons; (4) POMs are good ligands with multifunctional coordination sites.

This research is aimed at understanding the assembly, crystallography and functions of POMs-based materials. We use Waugh, Keggin, or Anderson POMs as building blocks, and transition-metal or lanthanide fragment as a linker, to construct seven novel compounds which exhibit interesting magnetic, luminescent, photochromic and adsorption properties. The prime results are as follows:

(1) By using transition-metal fragment as a linker, a sandwich tetracobalt(II) substituted tungstosilicate $K_{10}[Co_4(H_2O)_2(B\text{-}\alpha\text{-}SiW_9O_{34}H)_2]\cdot 21H_2O$ has been synthesized. This compound offers ideal structural supports for the study of the interactions between paramagnetic metal atoms as well as between delocalized electrons and paramagnetic metal atoms.

(2) By introducing lanthanide fragments, a series organic-inorganic hybrids based on Keggin tungstophosphates ($[Ln(NMP)_6(PW_{12}O_{40})_n]$ (NMP = *N*-methyl-2-pyrrolidone) (Ln = Pr, Eu, Gd) and $[Ln_2(NMP)_{12}(PW_{12}O_{40})][PW_{12}O_{40}]$ (Ln = Gd, Er)) have been synthesized. The compound $[Eu(NMP)_6(PW_{12}O_{40})_n]$ can be used as a Zn^{II}-selective sensor. The compound $[Gd_2(NMP)_{12}(PW_{12}O_{40})][PW_{12}O_{40}]$ has interesting photochromic properties and undergoes an unusual photo-induced single-crystal-to-single-crystal (SCSC) phase transformation.

(3) By using the Anderson-type anion and the lanthanide cation, we have constructed the simple but highly hydrophilic polyoxometalate $[Tm_2(H_2O)_{14}CrMo_6O_{24}H_6][CrMo_6O_{24}H_6]\cdot 16H_2O$ and reported its temperature-dependent SCSC phase transformation that occurs at surprisingly low temperature (< 113 K). Furthermore, this compound can undergo a few desorption and adsorption cycles.

In future work, we will base on the reported results to extend the research. The central plan is as follows:

(1) To investigate adsorption properties of $K_{10}[Co_4(H_2O)_2(B\text{-}\alpha\text{-}SiW_9O_{34}H)_2]\cdot 21H_2O$.

(2) To design novel photochromic system based on Keggin tungstophosphates.

(3) To complete syntheses and property studies of the series of compounds based on Anderson anion ($[CrMo_6O_{24}H_6]^{3-}$) and lanthanide cations.

Key Words: polyoxometalates; building blocks; crystallography; functional materials

Chapter 1 Overview

1.1 Background

Polyoxometalates (POMs) are nano-sized transition metal oxygen anion clusters, more specifically, they are oligomeric aggregates of metal cations (usually the d^0 species V(V), Nb(V), Ta(V), Mo(VI) and W(VI)) bridged by oxide anions that form by self-assembly processes [l−5]. They are a rapidly growing class of compounds. The first report of what we term a polyoxometalate dates back to Berzelius (1826), and more than 70 different elements have been so far reported as POMs constituents. The reported POMs can be divided into six basic types, Keggin, Silverton, Dawson, Anderson, Waugh and Lindqvist (Fig. 1).

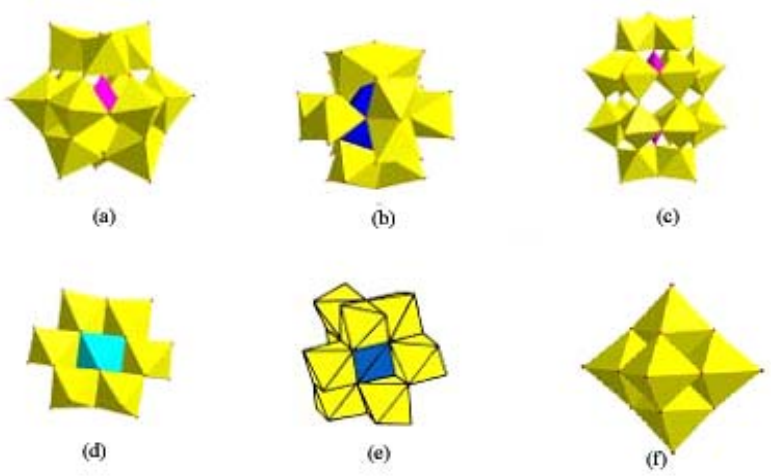

Fig. 1 Six basic types of POMs: (a) Keggin, (b) Silverton, (c) Dawson, (d) Anderson, (e) Waugh, (f) Lindqvist.

Owing to their sizes, structures, and properties, POMs are often referred to as soluble metal-oxide fragments and, as such, are receiving considerable attention. While their biological properties are the subject of increasing interest [6], catalysis [7−9] and materials science [10−13] are still the two main fields of applications of POMs today. POMs are attractive components for the design of advanced materials and devices [10−13], because

properties that are essential for applications in material science can be readily tailored in POMs through rational design [5, 14]. These properties include molecular composition, size, shape, charge density, redox potentials, acidity, and solubility.

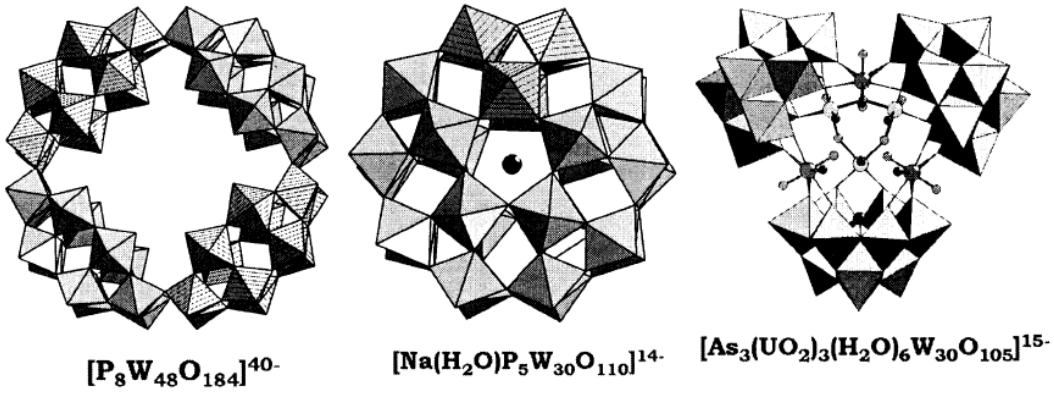

Fig. 2 The structures of a: $[P_8W_{48}O_{184}]^{40-}$, b: $[Na(H_2O)P_5W_{30}O_{110}]^{14-}$, c: $[As_3(UO_2)_3(H_2O)_6W_{30}O_{105}]^{15-}$

Small metal-oxygen polyoxometalates can serve as building blocks. Simple metal-oxygen building blocks can be linked together to form new structures. A large variety of linking units combined with the abundant building blocks provide the possibility of producing a wide range of POMs structures through various linking geometries. Fig. 2 shows structures of different shapes and sizes of POMs linked by smaller metal-oxygen POMs units. Four $\{P_2W_{12}\}$ building blocks are connected to each other to form an approximately ring shaped anion. The crystal structure of $\{P_8W_{48}\}$ reveals that the central cavity of the anion contains a number of potassium cations [15]. Structure of the anion $[Na(H_2O)P_5W_{30}O_{110}]^{14-}$ can regarded as a cyclic assembly of five $\{PW_6\}$ groups [16]. The central Na^+ can be replace other canons of similar size, e.g. Ca^+, most Ln^{III}, and U^{IV} [17, 18]. The central cation is coordinated by a H_2O molecule that is enclosed in the central cavity [19]. The sodium derivative has been evaluated as a catalyst for the oxidation of H_2S to sulfur, and was the best of the POMs examined [20]. The anion, $[(UO_2)_3(H_2O)_5As_3W_{29}O_{104}]^{19-}$ has the structure

shown in Fig. 2 which contains three $\{AsW_{10}\}$ fragments bridged by three pentagonal-bipyramidal $\{UO_2\}^{3+}$ cations [21].

Increasing attention is currently being paid to POMs in the domain of material science due to their chemical, structural and electronic versatility. The preparation of functional materials using polyoxometalates as nanoscale building blocks is a very rich area for research [22−33].

POM-based materials with magnetic properties:

The development of POM-based clusters incorporating paramagnetic centres is an interesting goal since it is possible to utilize existing building blocks/clusters to generate very large magnetic molecules. In fact, it has been shown that it is possible to substitute the $\{Mo_2\}$ 'linker' groups present in the Keplerate $(Pentagon)_{12}(Linker)_{30}$ species with Fe^{III} to yield a $\{Mo_{72}Fe_{30}\}$ cluster with the formula $[Mo_{72}Fe_{30}O_{252}(CH_3COO)_{10}\{Mo_2O_7(H_2O)\}\{H_2Mo_2O_8(H_2O)\}_3(H_2O)_{91}]$ (Fig. 3) [34]. This cluster is smaller than the parent $\{Mo_{132}\}$ with an outer diameter of *ca*. 24 Å and inner diameter of *ca*. 18 Å. Further, the $\{Mo_{72}Fe_{30}\}$ cluster is comprised of only Mo^{VI} atoms whereas the $\{Mo_{72}Mo_{30}\}$ cluster contains 36 reduced MoV centres (the 30 linking units are reduced and the remaining 6 centres are delocalised over the 12 pentagonal centres present in the cluster). The presence of the Fe(III) centres, combined with the weak antiferromagnetic exchange between these centres, means that there are 30 mainly uncorrelated spins at room temperature and the cluster therefore has a very large *S* (approaching 150/2). The Fe(III) centres of the cluster span an icosidodecahedron and the extremely rich and interesting magnetic properties have been investigated using the Heisenberg model [35]. In this respect the $\{Mo_{72}Fe_{30}\}$ has been termed as a mesoscopic paramagnet in which classical behavior extends down to extraordinarily low temperatures. Moving from Fe–Mo to Fe–Mo–V, the self-assembly of molybdate building units in the presence of Fe^{II} and V^{IV} produces the first

mixed-spin heterometal Keplerate-type clusters displaying ferrimagnetic interactions [36] where the clusters have the compostion: $\{(Mo^{VI})–Mo^{VI}_5\}_{12}M_{30}$ where M = V^{IV}, Fe^{III} [37]. Further, it appears that when large numbers of paramagnetic metal centres like 30 Fe^{III} or 20 VO^{2+} are integrated within their structure, extraordinary spin topologies can be realised on a discrete molecular level. Further functionalisation of these systems allows, e.g. to link them forming chains or layers in solid state reactions at room temperature [38].

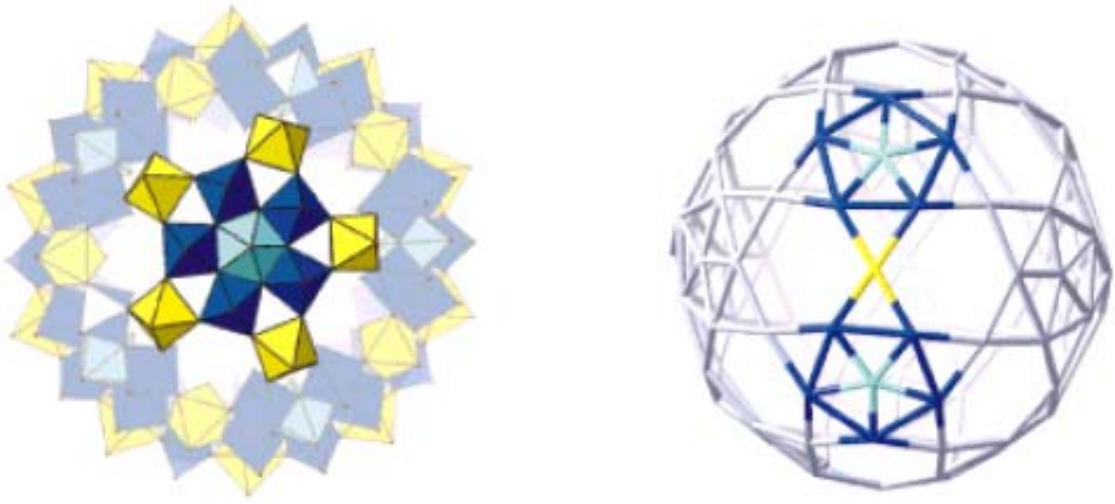

Fig. 3 polyhedral representation viewed along a C_5 axis showing five of the openings formed by the (Mo_9O_9) and ($Mo_3Fe_3O_6$) rings ({(Mo)Mo_5} units: blue; central MoO_7 unit: turquoise; linkers {Fe}: yellow).

POM-based materials with conducting properties:

The formation of hybrid materials based on POMs with stacks of partially oxidized p-electron donor molecules of tetrathiafulvalene (TTF) has been accomplished to yield conducting POM-based materials. This is interesting because the inorganic POM anion can act as a structural spacer unit, incorporate additional functionality such as a scaffold for paramagnetic ions or to act as an electron acceptor [30]. This area is progressing rapidly with the compounds based on [BEDT-TTF]$_5$[$H_3V_{10}O_{28}$] (Fig. 4) [39] and [BEDT-TTF]$_6$[Mo_8O_{26}] [40] (BEDT-TTF = bis(ethylenedithio)tetrathiafulvalene) which behave as metals down to 50

and 60 K with room temperature conductivities of 360 and 3 S cm^{-1}, respectively. In addition, a POM radical salt with metallic behavior down to 2 K has been synthesized [41]. The compound is based on $[BEDOTTF]_6K_2[BW_{12}O_{40}]$ and is formed from $[BW_{12}O_{40}]^{5-}$ and the organic radical (BEDO-TTF) (=bis(ethylenedioxo) tetrathiafulvalene). The realization of POM–organic conducting hybrids means that devices incorporating both POM clusters and organic conductors and polymers are also accessible. A chiral POM conductor has also been produced using the chiral cluster $[H_4Co_2Mo_{10}O_{38}]^{6-}$ electrocrystallised with (BEDT-TTF or ET) [31] and POM-based materials that have mobile lithium ions have also been realized [42].

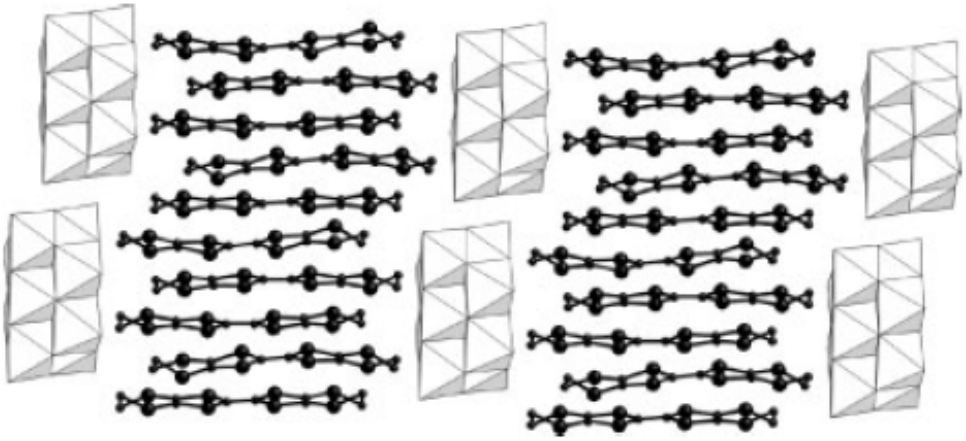

Fig. 4 Packing diagram of $[BEDT\text{-}TTF]_5[H_3V_{10}O_{28}]$ showing the alternating organic-inorganic layers.

POM-based materials with adsorption properties:

Polyoxometalates, which are nano-sized metal-oxide macroanions and show unique redox or acidic properties, can create molecular-sized spaces within them or in the solid state with the combination of appropriate cations [43–51]. As shown in Fig. 5, porous polyoxometalate compounds can be classified into three groups with regard to the location of the pores; compounds with pores in (a) the intercrystallite space [52–54], (b) the molecular structure of

polyoxometalates [55,56], and (c) the crystal lattice created by the arrangements of polyoxometalates and molecular cations (macrocations) [57–66]. As shown in Fig. 5a, $(NH_4)_3[PW_{12}O_{40}]$ is non-porous single crystal when synthesized at 473 K, while submicron-sized dodecahedron particle form by the self-organization of 5~10 nm nanocrystallites at 368K [53]. The crystallographic analysis of the single crystal shows that NH^{4+} and $[PW_{12}O_{40}]^{3-}$ are closely packed in the crystal lattice, and no pores exist. On the other hand, the dodecahedron particle shows type-I N_2 adsoption isotherm characteristic of compounds with micropores. The surface area (65 $m^2\ g^{-1}$) is larger than the outer surface area of the dodecahedron particle (4 $m^2\ g^{-1}$), and the calculated crystallite size is 10 nm. The electron diffraction of the dodecahedron particle shows discrete spots, indicating that the nanocrystallites are crystallographically ordered in the particles. Therefore, it is probable that the $(NH_4)_3[PW_{12}O_{40}]$ dodecahedron particle is formed by the self-organization of nanocrystallites and the micropores exist in the intercrystallite space. As shown in Fig. 5b, ring shaped or spherical nano-sized polyoxometalate clusters are formed by the self-organization of several tens to more than hundred molybdenum atoms in acidic solution with reducing reagents [55] or under UV irradiation [56]. Water of crystallization exists in the ring or sphere, and a part of the water molecules can be exchanged with amphiphilic molecules such as methanol and formic acid. The assembly of polyoxometalates (macroanions) and molecular cations (macrocations) can create ionic crystals with specific structures (Fig. 5c) [57–66]. By the control of the shape, size, and charge of the macroions, it is possible to predetermine their arrangement and to create molecular-sized spaces in the crystal lattice.

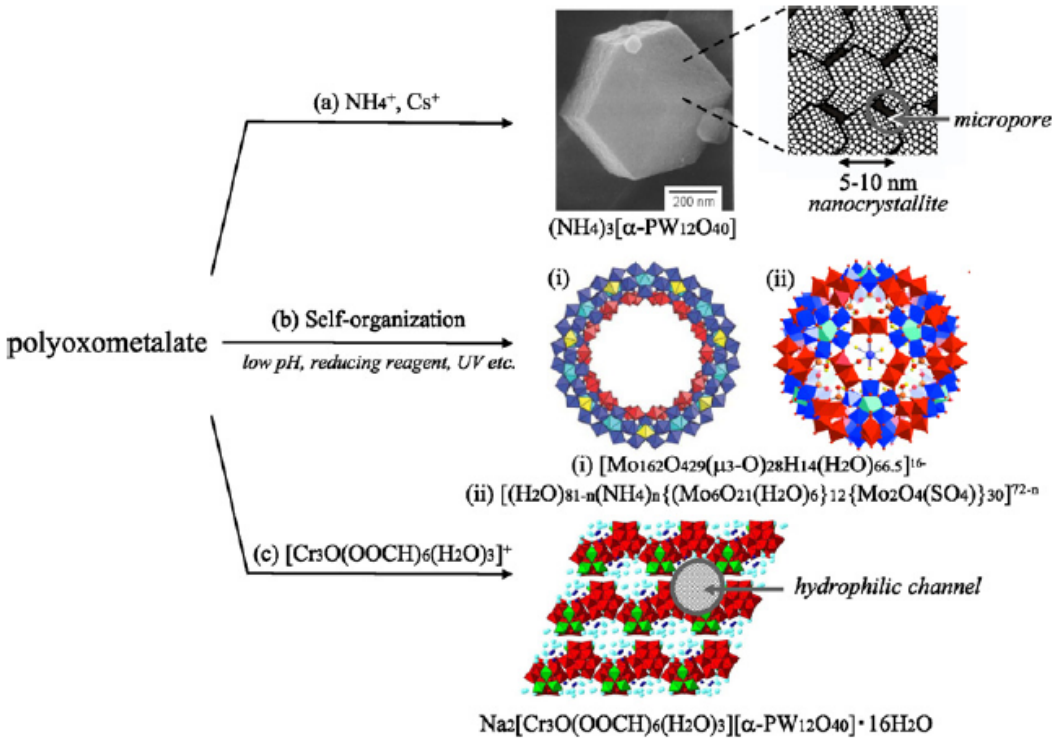

Fig. 5 Classification of porous polyoxometalate compounds: (a) NH_4^+; (b) self-organization; (c) $[Cr_3O(OOCH)_6(H_2O)_3]^+$.

1.2 Objectives

This research is aimed at understanding the assembly, crystallography and functions of POMs-based materials.

Assembly: by using POMs as building blocks, and transition-metal or lanthanide fragment as a linker, to design and fabricate different frameworks.

Crystallography: to grow crystals, and to explore the structures by single-crystal X-ray analysis.

Functions: to study their magnetic, optic, electronic, or adsorption properties.

The prime objectives are as follows:

(1) Using transition-metal fragment or rare-earth metal as a linker, to design and synthesize POMs-based magnetically interesting compounds.

(2) Using rare-earth metal as a linker to design POMs-based luminescent sensors.

(3) To synthesize POMs-based photochromic or electrochromic materials and investigate their functional mechanism.

(4) To study adsorption and selective adsorption properties of POMs-based materials.

References

[1] A. Müller, E. Krickemeyer, J. Meyer, H. Bögge, F. Peters, W. Plass, E. Diemann, S. Dillinger, F. Nonnenbruch, M. Randerath and C. Menke, *Angew. Chem., Int. Ed. Engl.*, 1995, **34**, 2122.

[2] A. Müller, E. Beckmann, H. Bögge, M. Schmidtmann and A. Dress, *Angew. Chem., Int. Ed.*, 2002, **41**, 1162.

[3] A. Müller and S. Roy, *Coord. Chem. Rev.*, 2003, **245**, 153.

[4] T. B. Liu, E. Diemann, H. L. Li, A. W. M. Dress and A. Müller, *Nature*, 2003, **426**, 59.

[5] C. L. Hill, *Chem. Rev.*, 1998, **98**, 1.

[6] (a) J. T. Rhule, C. L. Hill, D. A. Judd and R. F. Shinazi, *Chem. Rev.*, 1998, **98**, 327; (b) Y. Tajima, *Trends Inorg. Chem.*, 2004, **8**, 107; (c) B. Hasenknopf, *Front. Biosci.*, 2005, **10**, 275; (d) T. Yamase, *J. Mater. Chem.*, 2005, **15**, 4773.

[7] (a) I. V. Kozhevnikov, Catalysts for Fine Chemicals, vol. 2: Catalysis by Polyoxometalates, Wiley, Chichester, UK, 2002; (b) I. V. Kozhevnikov, *Chem. Rev.*, 1998, **98**, 171; (c) I. V. Kozhevnikov, *J. Mol. Catal. A: Chem.*, 2007, **262**, 86.

[8] N. Mizuno and M. Misono, *Chem. Rev.*, 1998, 98, 199. 11 (a) C. L. Hill, L. Delannoy, D. C. Duncan, I. A. Weinstock, R. F. Renneke, R. S. Reiner, R. H. Atalla, J. W. Han, D. A. Hillesheim, R. Cao, T. M. Anderson, N. M. Okun, D. G. Musaev and Y. V. Geletii, *C. R. Chim.*, 2007, **10**, 305; (b) C. L. Hill, *J. Mol. Catal. A: Chem.*, 2007, **262**, 2.

[9] (a) M. V. Vasylyev and R. Neumann, *J. Am. Chem. Soc.*, 2004, **126**, 884; (b) M. Vasylyev, D. Sloboda-Rozner, A. Aimov, G. Maayan and R. Neumann, *Top. Catal.*, 2005, **34**, 93; (c) R. Neumann and A. M. Khenkin, *Chem. Commun.*, 2006, 2529.

[10] T. Yamase, *Chem. Rev.*, 1998, **98**, 307.

[11] (a) E. Coronado and C. J. Gómez-García, *Chem. Rev.*, 1998, **98**, 273; (b) E. Coronado and J. R.

Galán-Mascarós, *J. Mater. Chem.*, 2005, **15**, 66; (c) E. Coronado, C. Giménez-Saiz and C. J. Gómez-García, *Coord. Chem. Rev.*, 2005, **249**, 1776; (d) E. Coronado and P. Day, *Chem. Rev.*, 2004, **104**, 5419.

[12] P. Gomez-Romero, Adv. Mater., 2001, 13, 163.

[13] (a) D. -L. Long and L. Cronin, *Chem.–Eur. J.*, 2006, **14**, 2698; (b) D. -L. Long, E. Burkholder and L. Cronin, *Chem. Soc. Rev.*, 2007, **36**, 105.

[14] P. Gouzerh and A. Proust, *Chem. Rev.*, 1998, **98**, 77.

[15] R. Contant and A. Teza, *Inorg. Chem.*, 1985, **24**, 4610.

[16] Y. Jeannin, *J. Cluster. Sci.*, 1992, **3**, 55.

[17] L Greaser, M. C. Heckel, R. J. Neitz and M. T. Pope, *Inorg. Chem.* 1993, **32**, 1573.

[18] M. R. Antonio and L. Soderholm, *J. Cluster Sci.*, 1996, **7**, 585

[19] M. H. Dickman, G. J. Gama, K. C. Kim and M. T. Pope, *J. Cluster Sci.*, 1996, **7**, 567.

[20] M. K. Harrup and C. L. Hill, *Inorg. Chem.*, 1994, 33, 5448.

[21] K. Kim and M. T. Pope, *J. Am. Chem. Soc.*, 1999, **121**, 8512.

[22] M. I. Khan, *J. Solid State Chem.*, 2000, **152**, 105.

[23] D. Volkmer, B. Bredenkotter, J. Tellenbroker, P. Kögerler, D. G. Kurth, P. Lehmann, H. Schnablegger, D. Schwahn, M. Piepenbrink and B. Krebs, *J. Am. Chem. Soc.*, 2002, **124**, 10489.

[24] S. Q. Liu, D. Volkmer and D. G. Kurth, *J. Cluster Sci.*, 2003, **14**, 405.

[25] G. Chaidogiannos, D. Velessiotis, P. Argitis, P. Koutsolelos, C. D. Diakoumakos, D. Tsamakis and N. Glezos, *Microelectron. Eng.*, 2004, **73–74**, 746.

[26] S. Q. Liu, H. Mohwald, D. Volkmer and D. G. Kurth, *Langmuir*, 2006, **22**, 1949.

[27] S. Q. Liu, D. G. Kurth, H. Mohwald and D. Volkmer, *Adv. Mater.*, 2002, **14**, 225.

[28] S. Q. Liu, D. Volkmer and D. G. Kurth, *Anal. Chem.*, 2004, **76**, 4579.

[29] S. Q. Liu, D. G. Kurth and D. Volkmer, *Chem. Commun.*, 2002, 976.

[30] E. Coronado, C. Gimenez-Saiz and C. J. Gomez-Garcia, *Coord. Chem. Rev.*, 2005, **249**, 1776.

[31] E. Coronado, S. Curreli, C. Gimenez-Saiz, C. J. Gomez-Garcia and J. Roth, *Synth. Met.*, 2005, **154**, 241.

[32] L. Xu, E. B. Wang, Z. Li, D. G. Kurth, X. G. Du, H. Y. Zhang and C. Qin, *New J. Chem.*, 2002, **26**,

782.

[33] M. Luban, F. Borsa, S. Bud'ko, P. C. Canfield, S. Jun, J. K. Jung, P. Kögerler, D. Mentrup, A. Müller, R. Modler, D. Procissi, B. J. Suh and M. Torikachvili, *Phys. Rev. B: Condens. Matter*, 2002, 66.

[34] A. Müller, S. Sarkar, S. Q. N. Shah, H. Bögge, M. Schmidtmann, S. Sarkar, P. Kögerler, B. Hauptfleisch, A. X. Trautwein and V. Schunemann, *Angew. Chem., Int. Ed.*, 1999, **38**, 3238.

[35] A. Müller, M. Luban, C. Schröder, R. Modler, P. Kögerler, M. Axenovich, J. Schnack, P. C. Canfield, S. Bud'ko and N. Harrison, *ChemPhysChem*, 2001, **2**, 517.

[36] B. Botar, P. Kögerler, A. Müller, R. Garcia-Serres and C. L. Hill, *Chem. Commun.*, 2005, 5621.

[37] A. Müller, A. M. Todea, J. van Slageren, M. Dressel, H. Bögge, M. Schmidtmann, M. Luban, L. Engelhardt and M. Rusu, *Angew. Chem., Int. Ed.*, 2005, **44**, 3857.

[38] A. Müller, P. Kögerler and A. W. M. Dress, *Coord. Chem. Rev.*, 2001, **222**, 193.

[39] E. Coronado, J. R. Galan-Mascaros, C. Gimenez-Saiz, C. J. Gomez-Garcia, E. Martinez-Ferrero, M. Almeida and E. B. Lopes, *Adv. Mater.*, 2004, **16**, 324.

[40] A. Lapinski, V. Starodub, M. Golub, A. Kravchenko, V. Baumer, E. Faulques and A. Graja, *Synth. Met.*, 2003, 138, 483.

[41] E. Coronado, C. Gimenez-Saiz, C. J. Gomez-Garcia and S. C. Capelli, *Angew. Chem., Int. Ed.*, 2004, 43, 3022.

[42] A. Dolbecq, C. du Peloux, A. L. Auberty, S. A. Mason, P. Barboux, J. Marrot, E. Cadot and F. Secheresse, *Chem. –Eur. J.*, 2002, **8**, 350.

[43] M. T. Pope and A. Müller, *Angew. Chem., Int. Ed. Engl.*, 1991, **30**, 34.

[44] C. L. Hill, C. M. Prosser-McCartha, *Coord. Chem. Rev.*, 1995, **143**, 407.

[45] T. Okuhara, N. Mizuno and M. Misono, *Adv. Catal.*, 1996, **41**, 113.

[46] C. L. Hill (Ed.), *Chem. Rev.*, 1998, **98**, 1, Special issue on polyoxometalate.

[47] T. Yamase and M. T. Pope (Eds.), Polyoxometalate Chemistry for Nano-Composite Design, Kluwer, Dordrecht, The Netherlands, 2002.

[48] I. V. Kozhevnikov, Catalysis by Polyoxometalates, Wiley, Chichester, UK, 2002.

[49] R. Neumann, in: J.E. Bäckvall (Ed.), Oxidation Methods, Wiley-VCH, Weinheim, 2004, 223.

[50] N. Mizuno, K. Kamata and K. Yamaguchi, Surface and Nanomolecular Catalysis, Taylor and Francis

Group, LLC, New York, 2006, 463.

[51] D. L. Long, P. Kogerler, L. J. Farrugia and L. Cronin, *Chem. Asian. J.*, 2006, **1**, 352.

[52] N. Mizuno and M. Misono, *Chem. Lett.*, 1987, 967.

[53] T. Ito, K. Inumaru and M. Misono, *J. Phys. Chem. B*, 1997, **101**, 9958.

[54] T. Okuhara, H. Watanabe, T. Nishimura, K. Inumaru and M. Misono, *Chem. Mater.*, 2000, **12**, 2230.

[55] A. Müller, S. Q. N. Shah, H. Bögge and M. Schmidtmann, *Nature*, 1999, **397**, 48.

[56] T. Yamase and P. V. Prokop, *Angew. Chem., Int. Ed.*, 2002, **41**, 466.

[57] M. Hölscher, U. Englert, B. Zibrowius and W. F. Hölderich, *Angew. Chem., Int. Ed. Engl.*, 1994, **33**, 2491.

[58] M. I. Khan, E. Yohannes and D. Powell, *Inorg. Chem.*, 1999, **38**, 212.

[59] D. Hagrman, P. J. Hagrman and J. Zubieta, *Angew. Chem., Int. Ed.*, 1999, **38**, 3165.

[60] J. H. Son, H. Choi and Y. U. Kwon, *J. Am. Chem. Soc.*, 2000, **122**, 7432.

[61] C. Du Peloux, A. Dolbecq, P. Mialane, J. Marrot, E. Rivière, F. Sécheresse, *Angew. Chem., Int. Ed.*, 2001, **40**, 2455.

[62] A. Forment-Aliaga, E. Coronado, M. Feliz, A. Gaita-Arĩno, R. Llusar and F. M. Romero, *Inorg. Chem.*, 2003, **42**, 8019.

[63] M. V. Vasylyev, R. Neumann, *J. Am. Chem. Soc.*, 2004, **126**, 884.

[64] Y. Ishii, Y. Takenaka and K. Konishi, *Angew. Chem., Int. Ed.*, 2004, **43**, 2702.

[65] S. S. Mal, U. Kortz, *Angew. Chem., Int. Ed.*, 2005, **44**, 3777.

[66] H. A. An, E. B. Wang, D. R. Xiao, Y. G. Li, Z. M. Su and L. Xu, *Angew. Chem., Int. Ed.*, 2006, **45**, 904.

Chapter 2 Sandwich magnetically interesting compounds built on Waugh POMs

2.1 Introduction

As the largest subclass of transitional metal substituted polyoxometalates (TMSPs), sandwich-type compounds have received increasing interest for their magnetism in recent years [1]. Though their structures containing more than one paramagnetic transition metal ion in close proximity may exhibit exchange-coupled spins leading to large spin ground states, these compounds often display the weak magnetism because the magnetic sites are encapsulated in a diamagnetic molecular metal oxide cluster [1c,1d]. As a matter of fact, the special use of these compounds in magnetism area is that they offer ideal structural supports for the study of the interactions between paramagnetic metal atoms [2,3] as well as between delocalized electrons and paramagnetic metal atoms [4].

On the other hand, it is to be noted that the interaction between orbitally degenerate ions, as for example high-spin cobalt(II) in octahedral sites, remains an essentially unsolved prob1em [5]. The high symmetry of sandwich-type TMSPs and the small distortion of the octahedral CoO_6 sites should facilitate the theoretical treatment required to give a quantitative explanation of the cobalt-cobalt magnetic interaction.

Herein, we report the synthesis, structure and magnetism of a sandwich TMSPs based on the magnetically interesting element Co and Waugh POMs $[B\text{-}\alpha\text{-}SiW_9O_{34}H]^{9-}$.

2.2 Results and discussion

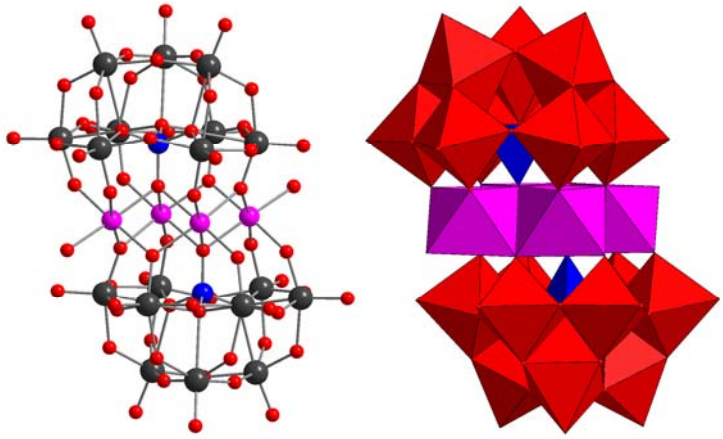

Fig. 1 Ball and stick (left) and polyhedral (right) representations of **1**. The color code is as follows: cobalt (purple), tungsten (black), silicon (blue), and oxygen (red).

Reaction of $CoCl_2 \cdot 6H_2O$ (0.2 mmol, 0.048 g) and $Na_9[\beta\text{-}SiW_9O_{34}H] \cdot 23H_2O$ [6] (0.1 mmol, 0.28 g) in 10 mL of KAc buffer (pH 4.8) at 80 °C for 1 h followed by slow evaporation at room temperature resulted in red single crystals (0.15 g, yield 54 %) [7]. X-ray analyses [8] reveal the compound, crystallized as $K_{10}[Co_4(H_2O)_2(B\text{-}\alpha\text{-}SiW_9O_{34}H)_2] \cdot 21H_2O$ (**1**), belongs to Monoclinic system. The dimeric polyoxoanion $[Co_4(H_2O)_2(B\text{-}\alpha\text{-}SiW_9O_{34}H)_2]^{10-}$ consists of two lacunary $[B\text{-}\alpha\text{-}SiW_9O_{34}H]^{9-}$ Keggin moieties linked by four Co^{2+} ions, leading to a sandwich-type structure with idealized C_{2v} symmetry (Fig. 1). The central belt of **1** is composed of a rhombic Co_4O_{16} group consisting of four coplanar CoO_6 octahedral sharing edges (Fig. 2). The distances of Co···Co along the sides of the rhombus are 3.18 Å while along the diagonal of the rhombus are 3.30 Å and 5.44 Å, respectively. There is a narrow variation in the Co-O-Co angles, with an average value of 95.8°. These values for the metal-metal separation and the geometry of the bridging unit are very similar to that found in the phosphorus-containing polyanion $[Co_4(H_2O)_2(\alpha\text{-}PW_9O_{34})_2]^{10-}$ which is the first example of sandwich TMSPs as well as of cobalt-based sandwich TMSPs reported by Weakley et al [9].

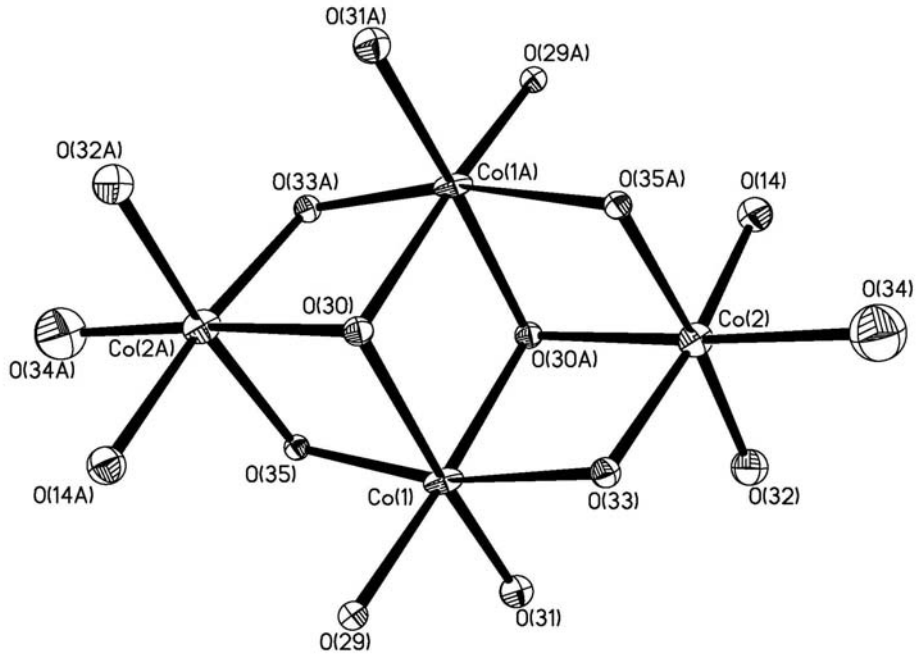

Fig. 2 ORTEP drawing of the central Co_4O_{16} fragment of **1**; thermal ellipsoids are drawn at the 30% probability level.

Although silicon-containing analogues **$SiMn_2W_9$**, **$SiCu_2W_9$**, and **$SiZn_2W_9$** had been well reported by Kortz et al, [1c] which were synthesized by reacting M^{2+} ions with $[\gamma\text{-}SiW_{10}O_{36}]^{8-}$ under conditions very similar to that used for the synthesis of **1**, we were not able to synthesize $[Co_4(H_2O)_2(B\text{-}\alpha\text{-}SiW_9O_{34}H)_2]^{10-}$ (**$SiCo_2W_9$**) starting from $[\gamma\text{-}SiW_{10}O_{36}]^{8-}$ under the same conditions. Interestingly, the reaction starting from $[\beta\text{-}SiW_9O_{34}H]^{9-}$ resulted in $[B\text{-}\alpha\text{-}SiW_9O_{34}H]^{9-}$ anions in compound **1**, which meant that the mechanism of the metal insertion reaction must be accompanied by isomerization ($[\beta\text{-}SiW_9O_{34}]^{10-} \rightarrow [B\text{-}\alpha\text{-}SiW_9O_{34}]^{10-}$). In our attempts to perform the reaction starting from $Na_{10}[\alpha\text{-}SiW_9O_{34}]$ [6], strangely, the crystals of the same compound could not be obtained. We speculated the $Na_{10}[\alpha\text{-}SiW_9O_{34}]$ synthesized according to Tézé's method was a mixture of $[A\text{-}\alpha\text{-}SiW_9O_{34}]^{10-}$ and $[B\text{-}\alpha\text{-}SiW_9O_{34}]^{10-}$, and thus caused the desired compound hard to be crystallized. Also deserving attention, despite the synthesis distinction between compound **1** and the three compounds (**$SiMn_2W_9$**, **$SiCu_2W_9$**, and **$SiZn_2W_9$**), they display the same anion

$[B\text{-}\alpha\text{-}SiW_9O_{34}]^{10-}$, which indicates that formation of the ($B\text{-}\alpha\text{-}SiW_9O_{34}$) fragment in a heated aqueous acidic medium is strongly favored.

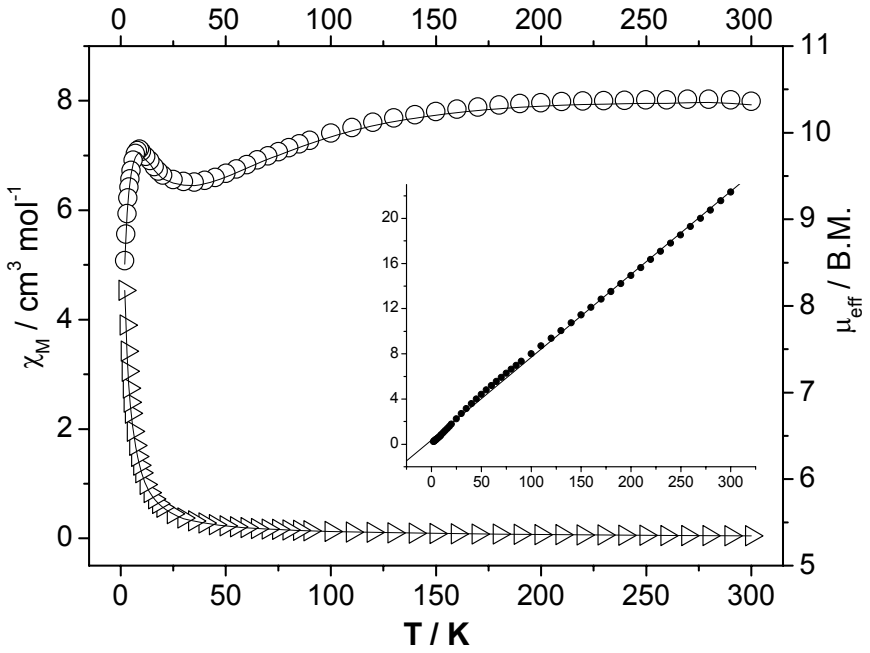

Fig. 3 χ_M (Δ) versus T and μ_{eff} (O) versus T plots for the compound **1**; the solid lines represent the theoretical values based on the equations.

Variable-temperature (2−300 K) magnetic susceptibility data at a magnetic field strength of 2 KG were collected for compound **1**. The χ_M and μ_{eff} versus T plots are shown in Fig. 3. The μ_{eff} at room temperature, 10.36 B.M., is larger than the spin-only value of 7.74 B.M. for the magnetically isolated high-spin octahedral Co_4 species due to the splitting of the $^4T_1$ term through spin-orbit coupling and local distortion of the octahedral sites. When the temperature is lowered, the value of μ_{eff} decreases smoothly, reaching a minimum at ca. 30 K (μ_{eff} = 9.43 B.M.). Below 30 K, the μ_{eff} increases smoothly upon cooling further and reaches a maximum with 9.81 B.M. at 9 K. After this maximum, the μ_{eff} value decreases quickly, with 8.52 B.M. at 2 K. All the data measured from 2 K to 300 K can be roughly fitted to a Curie–Weiss law with C = 13.62 cm^3 K mol^{-1} and θ = −4.86 K. Interestingly, here the plot of μ_{eff} versus T

looks like that found in some irregular spin state complexes [10]. To the best of our knowledge, the case has not been previously reported in other sandwich-type TMSPs. However, the magnetic mechanism of **1** is completely distinct from that of those irregular spin state compounds.

In order to explain the observed magnetic property of the title compound**,** the following exchange scheme has been used:

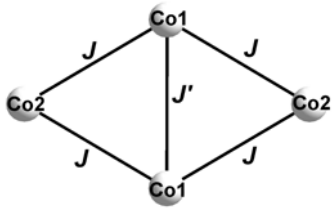

The interactions between the metal ions of the Co_4O_{16} unit can be described by two exchange coupling constants *J* and *J'*, where *J* represents the interactions along the sides of the rhombus while *J'* represents interactions along the short diagonal of the rhombus. As far as the existence of strong spin-orbit coupling for cobalt(II) ions was concerned, the magnetic data were analyzed by the following equations:

$$\chi_{tet} = \frac{Ng^2\beta^2}{3kT} \frac{\sum_i S_i(S_i+1)(2S_i+1)\exp(-E_i/KT)}{\sum_i (2S_i+1)\exp(-E_i/KT)}$$

$$\sum_i S_i(S_i+1)(2S_i+1)\exp(-E_i/kT) =$$

546EXP((−18*J*−24*J'*)/−*kT*)+330EXP((−6*J*−24*J'*)/−*kT*)+160EXP((4*J*−24*J'*)/−*kT*)+84EXP((12*J*−24*J'*)/−*kT*)+30EXP((18*J*−24*J'*)/−*kT*)+6EXP((22*J*−24*J'*)/−*kT*)+330EXP((−12*J*−24*J'*)/−*kT*)+180EXP((−2*J*−24*J'*)/−*kT*)+84EXP((6*J*−24*J'*)/−*kT*)+30EXP((12*J*−24*J'*)/−*kT*)+6EXP((16*J*−24*J'*)/−*kT*)+180EXP((−6*J*−24*J'*)/−*kT*)+84EXP((2*J*−24*J'*)/−*kT*)+30EXP((8*J*−24*J'*)/−*kT*)+84EXP((−24*J'*)/−*kT*)+330EXP((−12*J*−6*J'*)/−*kT*)+180EXP((−2*J*−6*J'*)/−*kT*)+120EXP((6*J*−6*J'*)/−*kT*)+30EXP((12*J*−6*J'*)/−*kT*)+6EXP((16*J*−6*J'*)/−*kT*)+160EXP((−8*J*−6*J'*)/−*kT*)+

114EXP((−6*J* ')/−*kT*)+6EXP((10*J*−6*J*')/−*kT*)+84EXP((−4*J*−6*J*')/−*kT*)+30EXP((2*J*−6*J*')/−*kT*)
+160EXP((−6*J*−2*J*')/−*kT*)+120EXP((2*J*−2*J*')/−*kT*)+30EXP((8*J*−2*J*')/−*kT*)+84EXP((−4*J*−2*J*'
)/−*kT*)+6EXP((6*J*−2*J*')/−*kT*)+30EXP((−2*J*−2*J*')/−*kT*)+6EXP((−2*J*')/−*kT*)+120

$$\sum_i (2S_i+1)\exp\left(-E_i/kT\right) =$$

13EXP((−18*J*−24*J*')/−*kT*)+11EXP((−6*J*−24*J*')/−*kT*)+9EXP((4*J*−24*J*')/−*kT*)+
7EXP((12*J*−24*J*')/−*kT*)+5EXP((18*J*−24*J*')/−*kT*)+3EXP((22*J*−24*J*')/−*kT*)+EXP((24*J*−24*J*')/−
kT)+11EXP((−12*J*−24*J*')/−*kT*)+9EXP((−2*J*−24*J*')/−*kT*)+7EXP((6*J*−24*J*')/−*kT*)+5EXP((12*J*−
24*J*')/−*kT*)+3EXP((16*J*−24*J*')/−*kT*)+9EXP((−6*J*−24*J*')/−*kT*)+7EXP((2*J*−24*J*')/−*kT*)+5EXP((
8*J*−24*J*')/−*kT*)+7EXP((−24*J*')/−*kT*)+11EXP((−12*J*−6*J*')/−*kT*)+9EXP((−2*J*−6*J*')/−*kT*)+
15EXP((6*J*−6*J*')/−*kT*)+6EXP((12*J*−6*J*')/−*kT*)+3EXP((16*J*−6*J*')/−*kT*)+9EXP((−8*J*−6*J*')/−*kT*)
+12EXP((−6*J*')/−*kT*)+3EXP((10*J*−6*J*')/−*kT*)+7EXP((−4*J*−6*J*')/−*kT*)+5EXP((2*J*−6*J*')/−*kT*)
+9EXP((−6*J*−2*J*')/−*kT*)+15EXP((2*J*−2*J*')/−*kT*)+5EXP((8*J*−2*J*')/−*kT*)+7EXP((−4*J*−2*J*')/−*kT*)
+3EXP((6*J*−2*J*')/−*kT*)+5EXP((−2*J*−2*J*')/−*kT*)+EXP((4*J*−2*J*')/−*kT*)+3EXP((−2*J*')/−*kT*)+16

$$\chi_{Lig} = \frac{N\beta^2}{3kT}\frac{3\left[3.15x+3.18+\left(2.84x+2.13\right)\exp\left(-3.75x\right)+\left(4.7x-6.05\right)\exp\left(-6x\right)\right]}{x\left[3+2\exp\left(-3.75x\right)+\exp\left(-6x\right)\right]}$$

$$(x=\lambda/kT)$$

$$\chi_M = \chi_{tet} + 4\chi_{Lig} - \frac{Ng^2\beta^2}{3kT}\left[4\times\frac{3}{2}\left(\frac{3}{2}+1\right)\right]$$

Best fitting for the experimental data leads to $J = -0.77$ cm^{-1}, $J' = 3.12$ cm^{-1}, $g = 2.34$, $\lambda = -129$ cm^{-1}, with the agreement factor $R = \sum(\chi_{obsd} - \chi_{cacld})^2 / \sum \chi_{obsd}^2 = 2.73 \times 10^{-4}$. The results reveal that magnetic interaction between Co1-Co1 is ferromagnetic while the Co1-Co2 interaction is antiferromagnetic. The exchange interactions in the compound are slightly

different from that found in the silicon-containing analogues $[\{SiM_2W_9O_{34}(H_2O)\}_2]^{12-}$ (M = Mn^{2+}, Cu^{2+}) [1c], in which the central Mn_4 unit exhibits antiferromagnetic ($J = -1.77(5)$ cm^{-1}) as well as weak ferromagnetic ($J' = 0.08(2)$ cm^{-1}) Mn-Mn exchange interactions and the Cu-Cu exchange interactions are antiferromagnetic ($J = -0.10(2)$ cm^{-1}, $J' = -0.29(2)$ cm^{-1}). It is believed that the major structural factors affecting exchange coupling in these compounds are the polyoxometalate matrixes since the polyoxometalate matrix may be considered a diamagnetic host encapsulating and thereby isolating magnetic clusters of transition metals.

2.3 Summary

In summary, we have synthesized a sandwich tetracobalt(II) substituted tungstosilicate which displays interesting isomerization ($[\beta\text{-}SiW_9O_{34}]^{10-} \rightarrow [B\text{-}\alpha\text{-}SiW_9O_{34}]^{10-}$). The magnetism has been studied based on an isotropic Heisenberg model supplemented by a zero-field splitting term. It must be noted that it is an approximate method and usually insufficient for cobalt(II) exchange system due to the existence of spin anisotropy, and it is still a great challenge to well-understand the cobalt magnetism.

References

[1] (a) U. Kortz, S. Nellutla, A. C. Stowe, N. S. Dalal, J. van Tol and B. S. Bassil, *Inorg. Chem.*, 2004, **43**, 144; (b) S. Nellutla, J. van Tol, N. S. Dalal, L. -H. Bi, U. Kortz, B. Keita, L. Nadjo, G. A. Khitrov and A. G. Marshall, *Inorg. Chem.*, 2005, **44**, 9795. (c) U. Kortz, S. Isber, M. H. Dickman, D. Ravot, *Inorg. Chem.*, 2000, **39**, 2915; (d) C. J. Gómez-García, E. Coronado, P. Gómez-Romero and N. Casañ-Pastor, *Inorg. Chem.*, 1993, **32**, 3378.

[2] G. F. Kokoszka, F. Padula, A. S. Goldstein, E. L. Venturini, L. Azevedo and A. R. Sidle, *Inorg. Chem.*, 1988, **27**, 59.

[3] (a) V. E. Simmons, Doctoral Dissertation, Boston University, 1963; Diss. Absrr. 1963, **24**, 1391; (b) L. C. W. Baker, V. E. S. Baker, S. H. Wasfi, G. A. Candela and A. H. Kahn, *J. Am. Chem. Soc.*, 1972, **94**, 5499; (c) L. C. W. Baker, V. E. S. Baker, S. H. Wasfi, G. A. Candela and A. H. J. Kahn, *Chem. Phys.*,

1972, **56**, 4917.

[4] N. Casañ-Pastor, Doctoral Dissertation, Georgetown University, 1988.

[5] O. Kahn, *Struct. Bonding*, 1987, **68**, 89.

[6] G. Hervé and A. Tézé, *Inorg. Chem.*, 1977, **16**, 2115.

[7] IR: 987, 951, 904, 876, 850, 757, 723, 532, 512, 486 cm^{-1}. Anal. Calcd (Found): K 7.1 (7.2), Co 4.3 (4.4), W 60.2 (59.7), Si 1.0 (1.1).

[8] Crystal data for the compound: $Co_4H_{48}K_{10}O_{91}Si_2W_{18}$, M_r = 5496.58, monoclinic, *P*2(1)/n, a = 12.296 (3) Å, b = 21.285(6) Å, c = 15.792(4) Å, α = 90° , β = 92.208(5)°, γ = 90°, V = 4130(2) $Å^3$, Z = 2, ρ_{calcd} = 4.420 g cm^{-3}, $2\theta_{max}$ = 26.39° ($-12 \le h \le 15$, $-26 \le k \le 23$, $-19 \le l \le 19$), T = 294(2) K, F(000) = 4868, GOF = 0.975, R_1 = 0.0576, wR_2 = 0.1492. CSD 416730.

[9] T. J. R. Weakley, H. T. jun. Evans, J. S. Showell, G. F. Tourné and C. M. Tourné, *J. Chem. Soc., Chem. Commun.*, 1973, 139.

[10] (a) E. -Q. Gao, J. -K. Tang, D. -Z. Liao, Z. -H. Jiang, S. -P. Yan and Q. -L. Wang, *Inorg. Chem.*, 2001, 40, 3134; (b) J. Tercero, C. Diaz, J. Ribas, M. Maestro, J. Mahĺa and H. Stoeckli-Evans, *Inorg. Chem.*, 2003, **42**, 3366; (c) Q. -L. Wang, L. -N. Zhu, D. -Z. Liao, S. -P. Yan, Z. -H. Jiang, P. Cheng and G.-M. Yang, *J. Mol. Struct.*, 2005, **754**, 10.

Chapter 3 Photochromic lanthanide compounds built on Keggin POMs

3.1 Syntheses, structures and properties of $[Pr(NMP)_6(PW_{12}O_{40})]_n$, $[Eu(NMP)_6(PW_{12}O_{40})]_n$ and $[Er_2(NMP)_{12}(PW_{12}O_{40})][PW_{12}O_{40}]$

3.1.1 Introduction

Polyoxometalates (POMs) are nano-sized metal-oxygen cluster species with a diverse compositional range and an enormous structural variety [1−3]. It is well-known that one of the most important properties of POMs is the capability to accept various numbers of electrons giving rise to mixed-valency colored species (heteropolyblues or heteropolybrowns) [4], which makes them suitable for photochromic and electrochromic materials [4−6]. Since the investigation of inorganic-organic hybrid materials became an expanding field, the preparation, microstructure, and photochromic process of POMs-based hybrid composites have been extensively investigated [7−11].

On the other hand, the rational design and synthesis of inorganic-organic hybrid architectures based on POMs and various metal coordination complexes are of considerable interest and of great challenge in current synthetic chemistry [12−23]. Comparing with large numbers of POMs-based hybrid materials structurally modified by transition-metal elements [12−20], rare-earth elements as the linkers have been paid less attention in assisting the self-assembly of POMs building blocks [21−23], although their compounds may possess potential applications in many fields. In most cases, it appears that oxygen atoms on the surface of POMs are rather reactive and are easily combined with the highly oxophilic rare earth ions to form precipitates instead of crystals. The introduction of protecting organic

ligands may be one of the effective methods to inhibit precipitation by coordinating rare earth ions and decreasing their highly oxophilic properties [23].

Herein, by using the protecting ligand *N*-methyl-2-pyrrolidone (NMP), three lanthanide-linked photochromic hybrids based on $[PW_{12}O_{40}]^{3-}$ have been successfully synthesized. Their photochromic, magnetic and luminescent properties have been investigated.

3.1.2 Experimental

1. Materials and methods

All reagents were purchased commercially and used without further purification. Elemental analyses (C, H, N) were conducted on a Perkin-Elmer 240C analyzer. Infrared spectra were obtained from a sample powder palletized with KBr on Nicolet AVATAR 360 FTIR spectrophotometer over the range 4000−400 cm^{-1}. UV spectra were obtained on a Unican UV-500 spectrometer (distilled water as solvent) in the range of 190−1100 nm. Variable temperature susceptibility measurements were carried out in the temperature range 2−300 K at a magnetic field strength of 2 kG with a Quantum Design MPMS-7 SQUID magnetometer. Diamagnetic corrections were made with Pascal's constants for all the constituent atoms. The emission spectra in an aqueous solution were recorded on a Cary Eclipse luminescence spectrophotometer.

2. Synthesis of $[Pr(NMP)_6(PW_{12}O_{40})]_n$ (**1**)

Reaction of $H_3PW_{12}O_{40}{\cdot}nH_2O$ (1.3 g), $PrCl_3{\cdot}6H_2O$ (0.142 g, 0.4 mmol) and *N*-methyl-2-pyrrolidone (0.5 mL) in an acetonitrile/water (2:1, v/v) mixed solution (10 mL) at 90 °C for 1 h followed by slow evaporation at room temperature in the dark resulted in colorless single crystals. Yield: 1.18 g (82 %). Anal. Calcd (%): C 10.0, H 1.5, N 2.3; Found: C 10.4, H 1.6, N 2.1. IR (KBr, *v*): 3404 (s), 2936 (w), 1640(vs), 1516 (m), 1406 (w), 1308

(w), 1262 (w), 1256 (m), 1080 (vs), 985 (vs), 896 (vs), 813 (vs), 521(m) cm^{-1}. UV-vis (solid-state, λ_{max}): 250 nm.

3. Synthesis of $[Eu(NMP)_6(PW_{12}O_{40})]_n$ (**2**)

2 was prepared according to the procedure described for **1** but using $EuCl_3 \cdot 6H_2O$ (0.147 g, 0.4 mmol) as the rare earth reagent. Yield: 1.12 g (77 %). Anal. Calcd (%): C 9.9, H 1.5, N 2.3; Found: C 10.1, H 1.7, N 2.1. IR (KBr, *v*): 3404 (s), 2937 (w), 1639(vs), 1513 (m), 1406 (w), 1308 (w), 1260 (w), 1258 (m), 1080 (vs), 983 (vs), 895 (vs), 813 (vs), 521(m) cm^{-1}. UV-vis (solid-state, λ_{max}): 250 nm.

4. Synthesis of $[Er_2(NMP)_{12}(PW_{12}O_{40})][PW_{12}O_{40}]$ (**3**)

3 was prepared according to the procedure described for **1** but using $ErCl_3 \cdot 6H_2O$ (0.153 g, 0.4 mmol) as the rare earth reagent. Yield: 1.15 g (79 %). Anal. Calcd (%): C 9.9, H 1.5, N 2.3; Found: C 10.3, H 1.4, N 2.2. IR (KBr, *v*): 3402 (s), 2940 (w), 1634(vs), 1517 (m), 1403 (w), 1310 (w), 1260 (w), 1256 (m), 1078 (vs), 980 (vs), 895 (vs), 810 (vs), 516(m) cm^{-1}. UV-vis (solid-state, λ_{max}): 250 nm.

5. Crystal structure determination

Structural measurements of three complexes were performed on a computer controlled Bruker SMART 1000 CCD diffractometer equipped with graphite-monochromated Mo-*Kα* radiation with radiation wavelength 0.71073 Å by using the *ω*-scan technique. Lorentz polarization and absorption corrections were applied. The structures were solved by direct methods using the program SHELX 97 and subsequent Fourier difference techniques, and refined anisotropically by full-matrix least-squares on F^2 using SHELXL 97. The summary of crystallographic data is given in Table 1.

Table 1 Crystal data and structure refinement for compounds **1**, **2** and **3**.

Compound	**1**	**2**	**3**
Empirical formula	$C_{30}H_{54}N_6O_{46}PPrW_{12}$	$C_{30}H_{54}N_6O_{50}PEuW_{12}$	$C_{60}H_{108}Er_2N_{12}O_{92}P_2W_{24}$
M_r	3612.87	3623.92	7278.44
T (K)	294(2)	294(2)	294(2)
λ (Å)	0.71073	0.71073	0.71073
Crystal system	Monoclinic	Monoclinic	Triclinic
Space group	$C2/c$	$C2/c$	$P\bar{1}$
a (Å)	22.021(3)	21.979(3)	12.1107(18)
b (Å)	12.9042(19)	12.7848(17)	13.592(2)
c (Å)	24.288(4)	24.310(3)	22.219(3)
α (°)	90	90	80.242(2)
β (°)	106.823(2)	107.303(2)	85.464(2)
γ (°)	90	90	67.550(3)
V (Å^3)	6606.4(16)	6522.2(15)	3330.9(9)
Z	4	4	1
D_c (g/cm^3)	3.632	3.691	3.629
F (000)	6424	6440	3230
$2\theta_{max}$ (°)	50.02	50.02	50.04
R_{int}	0.0648	0.0652	0.0399
GOF on F^2	1.011	1.067	1.072
$R1$	0.0429	0.0602	0.0645
$wR2$	0.1095	0.1620	0.1636

Crystallographic data (excluding structure factors) for the structural analysis have been deposited with the Cambridge Crystallographic Data Centre, CCDC nos. 294255, 611820 and 611432 for structures of the three compounds. Copies of this information may be obtained free of charge from The Director, CCDC, 12 Union Road, Cambridge, CB2 1EZ, UK (fax: +44 1223 336 033; e-mail: deposit@ccdc.cam.ac.uk or www: http://www.ccdc.cam.ac.uk).

3.1.3 Results and discussion

X-ray analyses reveal that **1** and **2** are isomorphous. The two compounds, crystallized as $[Ln(NMP)_6(PW_{12}O_{40})]_n$ (Ln = Pr (**1**), Eu (**2**)), consist of 1D infinite zigzag chains built from alternate polyanions and $[Ln(NMP)_6]^{3+}$ subunits, displaying a $\{(anion)M\text{-}donor\}_n$ (M = Ln; anion = $PW_{12}O_{40}^{3-}$; donor = NMP) type of structure (Fig. 1). The adjacent Ln···Ln distances are 15.540 Å for **1** and 15.442 Å for **2**, respectively. The coordination polyhedron of Ln^{III} can

be represented as a distorted, bicapped trigonal prism (Fig. 2). In **1**, the Pr−O bond lengths are within the range from 2.326 to 2.579 Å (mean value 2.414 Å). The torsion angle between the top plane and the bottom plane is 7.52 °. In **2**, the Eu−O bond lengths are within the range from 2.256 to 2.503 Å (mean value 2.355 Å). The torsion angle between the top plane and the bottom plane is 7.66 °.

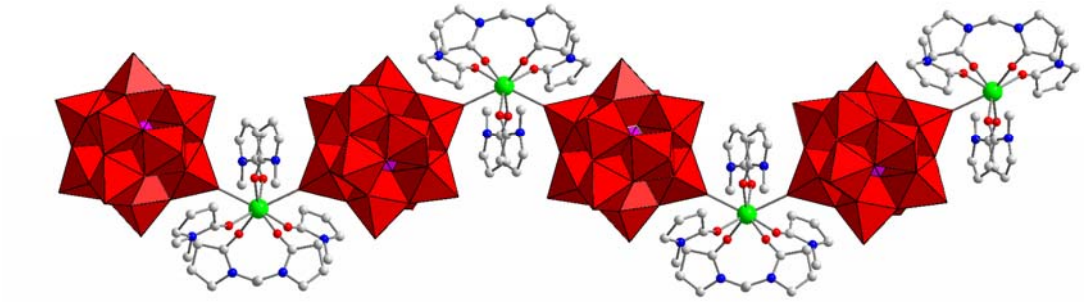

Fig. 1 Ball and stick and polyhedral representations of the 1D infinite zigzag chain structure of compound **1** (compound **2** is isomorphous to **1**). The color code is as follows: Pr (green), O (red), N (blue), C (gray), WO_6 (red), PO_4 (purple).

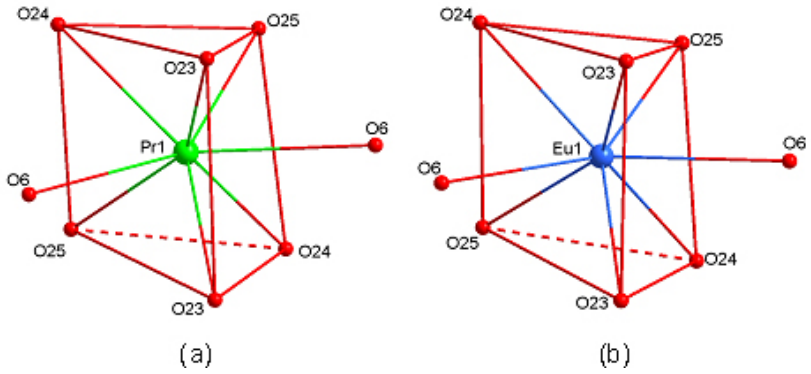

Fig. 2 a) Coordination polyhedron around Pr^{III} in **1**; b) Coordination polyhedron around Eu^{III} in **2**. Bond lengths (Å): a) Pr(1)−O(6), 2.579(10); Pr(1)−O(23), 2.364(12); Pr(1)−O(24), 2.387(13); Pr(1)−O(25), 2.326(13); b) Eu(1)−O(6), 2.503(3); Eu(1)−O(23), 2.305(2); Eu(1)−O(24); 2.357(2); Eu(1)−O(25), 2.256(2).

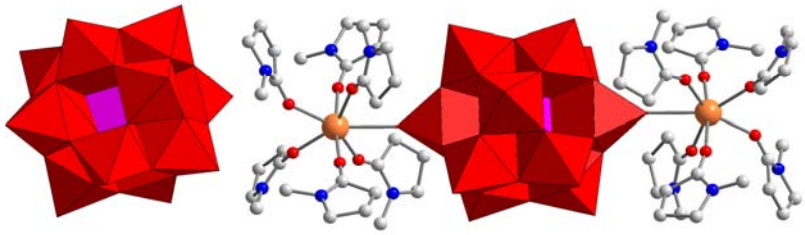

Fig. 3 Ball and stick and polyhedral representations of the ionic asymmetric structure of compound **3**. The color code is as follows: Er (orange), O (red), N (blue), C (gray), WO_6 (red), PO_4 (purple).

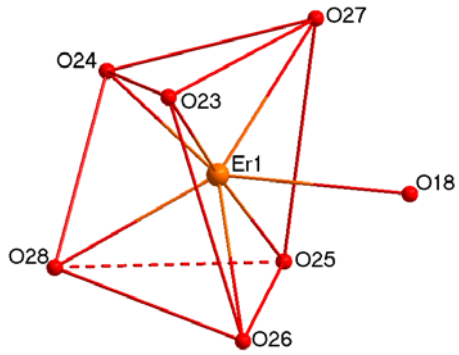

Fig. 4 Coordination polyhedron around Er^{III} in **3**. Bond lengths (Å): Er(1)−O(18), 2.416(15); Er(1)−O(23), 2.18(2); Er(1)−O(24), 2.234(19); Er(1)−O(25), 2.192(19); Er(1)−O(26), 2.343(18); Er(1)−O(27), 2.254(18); Er(1)−O(28), 2.236(18).

Interestingly, different from **1** and **2**, compound **3** exhibits an ionic, asymmetric structure probably because of the lanthanide contraction. Compound **3** consists of the $[PW_{12}O_{40}]^{3-}$ anion and the $[Er_2(NMP)_{12}(PW_{12}O_{40})]^{3+}$ cation in which either of Er^{III} ions is coordinated with 6 NMP molecules and connected by $[PW_{12}O_{40}]^{3-}$ (Fig. 3). The adjacent Er···Er distance is 15.353 Å. The coordination polyhedron of Er^{III} can be represented as a highly distorted, single-capped trigonal prism (Fig. 4).The Er−O bond lengths are within the range from 2.18 to 2.416 Å (mean value 2.265 Å). The torsion angle between the top plane and the bottom plane is 28.42 °.

When exposed to sunlight, colorless crystals of **1**−**3** can turn deep blue gradually. This observation should be attributed to the electron transfer between electron donors of organic molecules and electron acceptors of polyoxometalate anions. The final result is that W^{VI} atoms of the polyanions are reduced and mixed-valence compounds are formed, leading to the observed photochromism [4]. As shown in Fig. 5, after irradiation with sunlight, the absorption band at 700 nm in visible region appeared due to metal-to-metal extra intervalence charge transfer (IVCT) ($W^{5+} \rightarrow W^{6+}$) [1]. The photochromic mechanism of **1**−**3** should be similar to that well-reported in charger-transfer alkylammonium-polyoxometalates [4]. The reasonable mechanism should involve the absorption of photons by the Keggin structure, resulting in the generation of an electron-hole pair which directly oxidizes NMP into NMP^{+}.

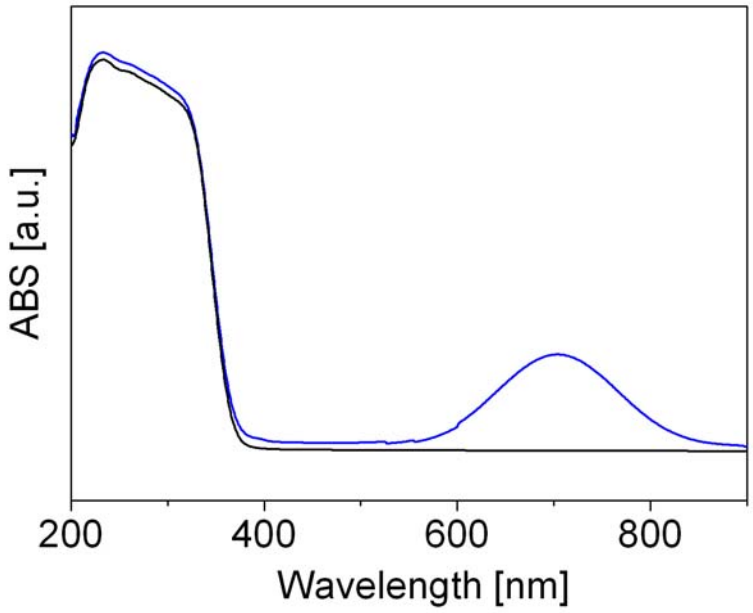

Fig. 5 The solid-state UV-vis spectra for compound **2** before (black curve) and after (blue curve) irradiation with sunlight.

Variable-temperature (2−300 K) magnetic susceptibility data at a magnetic field strength of 2 kG were collected for compound **1** (Fig. 6). The μ_{eff} value at room temperature was 3.52 B.M., which is slightly lower than that expected, 3.58 B.M., per insulated Pr(III) ion in the

$^3H_4$ ground state (g = 4/5). As far as the existence of a strong spin-orbit coupling for Ln atoms is concerned, the magnetic data were analyzed by the following approximate treatment equations previously derived by McPherson et al [24].

$$\chi_{\mathrm{Pr}} = \frac{Ng^2\beta^2}{kT}\frac{2\exp(-\Delta/kT)+8\exp(-4\Delta/kT)+18\exp(-9\Delta/kT)+32\exp(-16\Delta/kT)}{1+2\exp(-\Delta/kT)+2\exp(-4\Delta/kT)+2\exp(-9\Delta/kT)+2\exp(-16\Delta/kT)}$$

$$\chi_{total} = \chi_{\mathrm{Pr}}/[1-\chi_{\mathrm{Pr}}(zJ'/Ng^2\beta^2)]$$

In expressions, Δ is the zero-field-splitting parameter. zJ' is the intermolecular magnetic coupling parameter. Best fitting for the experimental data leads to Δ = − 0.910 cm^{-1}, zJ' = −4.719 cm^{-1}, g = 0.806, and $R = \sum(\chi_{\mathrm{obsd}} - \chi_{\mathrm{cacld}})^2 / \sum(\chi_{\mathrm{obsd}})^2 = 1.73 \times 10^{-3}$.

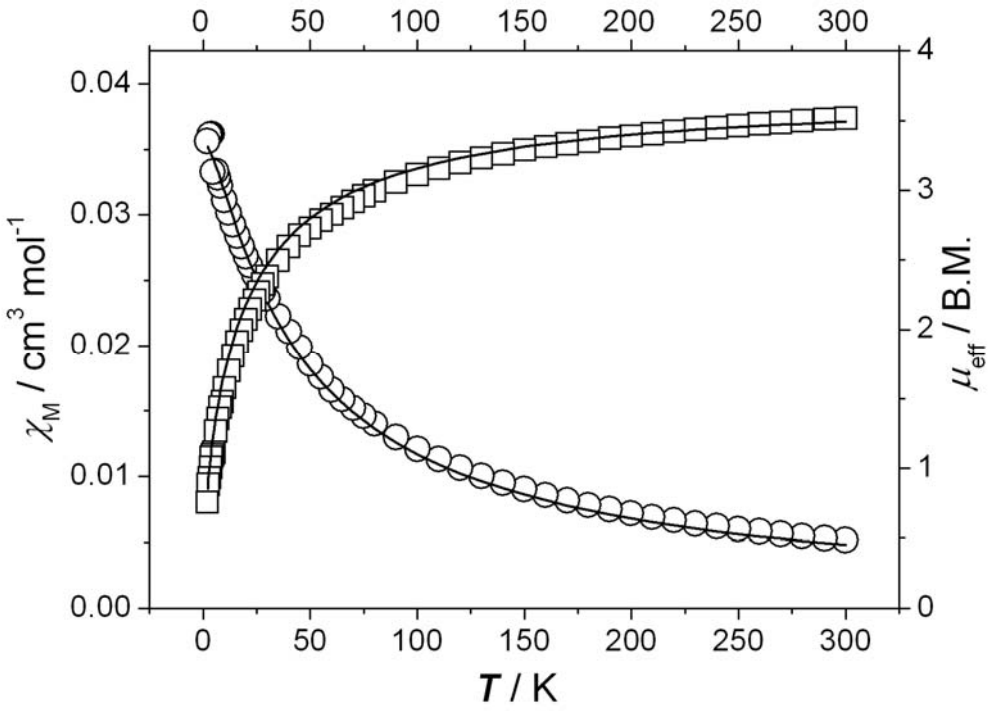

Fig. 6 χ_M (O) vs T and μ_{eff} (□) vs T plots for compound **1**. The solid lines represent the theoretical values based on the equations.

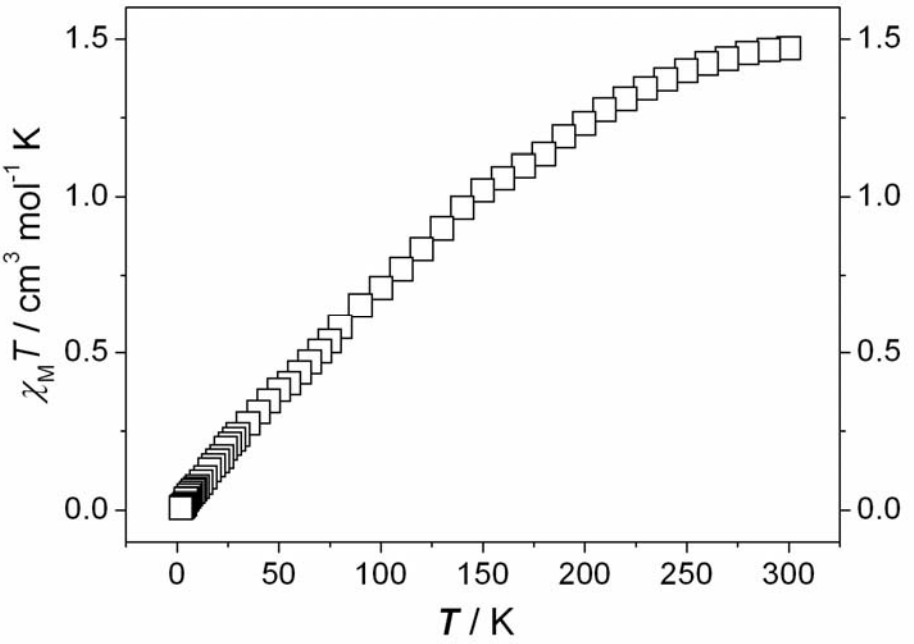

Fig. 7 $\chi_M T$ (□) vs T plots for compound **2**.

Variable-temperature (2−300 K) magnetic susceptibility data at a magnetic field strength of 2 kG were collected for compound **2** (Fig. 7). At room temperature, the observed $\chi_M T$ value of **2** is *ca*. 1.47 cm^3 mol^{-1} K, slightly less than the value 1.5 for a Eu(III) ion calculated by Van Vleck equation allowing for population of the excited state with higher values of J at 293 K [25]. As the temperature is lowered, $\chi_M T$ decreases continuously as a result of the depopulation of the depopulation of the levels with nonzero J values. At the lowest temperature, $\chi_M T$ is close to zero, indicating a $J = 0$ ground state of the Eu(III) ion ($^7F_0$).

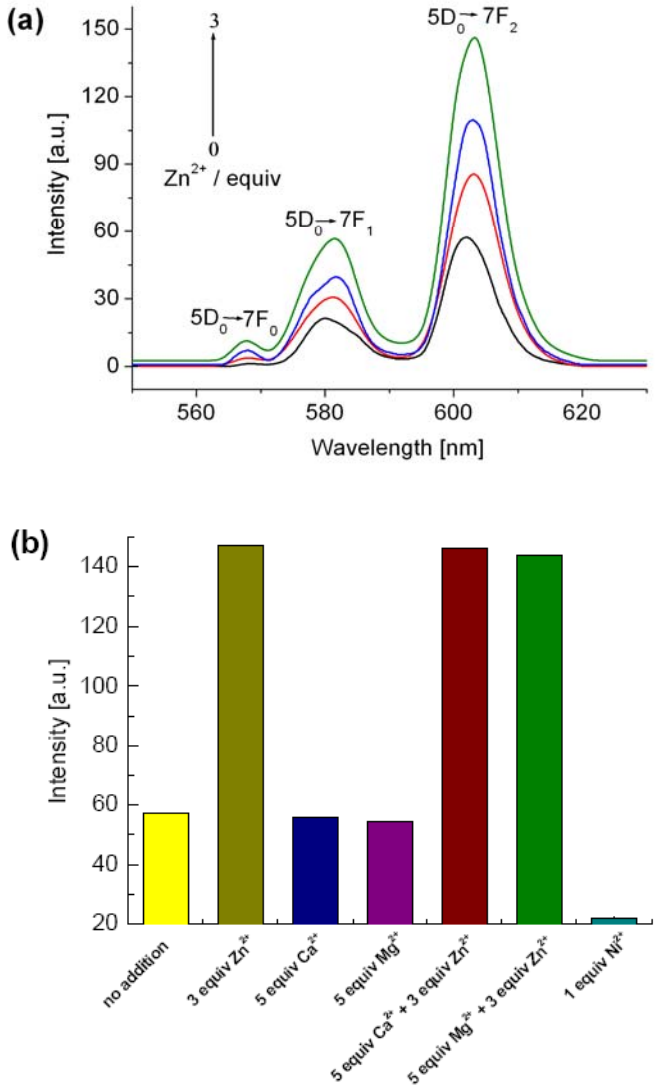

Fig. 8 a) Emission spectra of compound **2** in an aqueous solution (5×10^{-3} M) at room temperature (excited at 289 nm) upon addition of ~ 0-3 equiv of Zn^{2+} ions, respectively: black, no addition; red, 1 equiv; blue, 2 equiv; green, 3 equiv; b) Luminescent intensity of the compound at 603 nm in aqueous solution at room temperature upon addition of Zn^{2+}, Ca^{2+}, Mg^{2+} or Ni^{2+} ions (excited at 289 nm). Cations were added as $ZnCl_2$, $CaCl_2$, $MgCl_2$ or $NiCl_2$.

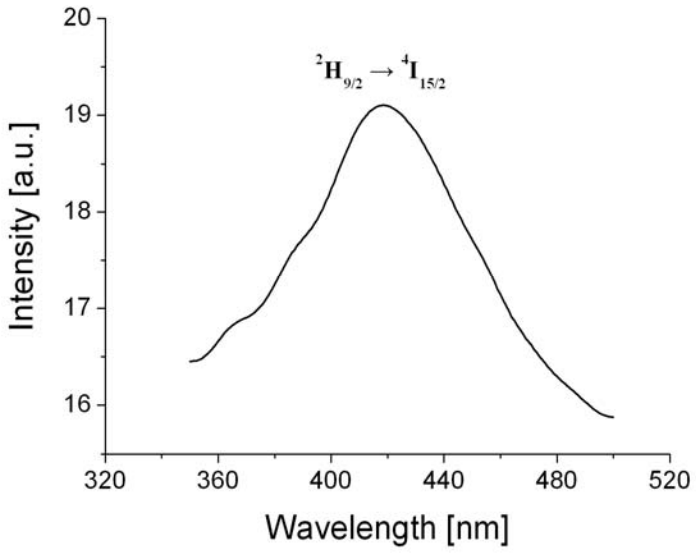

Fig. 9 Emission spectra of **3** (5×10^{-3} M) at room temperature (excited at 320 nm) in an aqueous solution.

The emission spectrum of **2** (Fig. 8a) at room temperature in an aqueous solution excited at 289 nm exhibited the characteristic transition of the Eu^{3+} ion: $^5D_0\rightarrow{}^7F_J$ (J = 0, 1, 2) [26]. Interestingly, upon addition of 1−3 equiv of Zn^{2+} gradually, the emission intensity of **1** obviously increased. The highest peak at 603 nm is closely thrice as intense as the corresponding band in the solution without Zn^{2+}. However, when the same experiments were performed for the introduction of Ca^{2+} and Mg^{2+} into the system, even the presence of 5 equiv of Ca^{2+} or Mg^{2+} in aqueous solution of **1** had no effect on the luminescent intensities either (Fig. 8b). While adding 1−3 equiv of transition metal ions such as Ni^{2+}, Co^{2+}, Mn^{2+} and Fe^{2+} to the solution of the compound, the luminescent intensities decreased or quenched (Fig. 8b). The above results imply that compound **2** could monitor or recognize Zn^{2+} to some extent and be considered as luminescent probes.

The emission spectra of **3** (Fig. 9) at room temperature in aqueous solution excited at 320 nm exhibited an intense band at about 425 nm, which was assigned to the emission of $^2H_{9/2}\rightarrow{}^4I_{15/2}$ [27]. Upon addition of Zn^{2+}, Ca^{2+} or Mg^{2+} to perform the same experiments to

compound **2**, however, the emission intensity of **3** had no effect, only decreased or quenched when transition ions were added. The results indicate that the Zn^{II}-selective sensor properties in this system might be connected with the central lanthanide ions.

3.1.4 Summary

In summary, a series of inorganic-organic hybrids built on Keggin tungstophosphates have been prepared. Compounds **1** and **2** exhibit 1D infinite zigzag chain structures, while compound **3** exhibits an ionic asymmetric structure due to lanthanide contraction. Their photochromic, magnetic and luminescent properties have been well studied. Especially, compound **2** displays an interesting luminescent selectivity for Zn^{2+} ions.

References

[1] M.T. Pope, Heteropoly and Isopoly Oxometalates, Springer-Verlag, Berlin, 1983.

[2] M.T. Pope and A. Müller, *Angew. Chem., Int. Ed.*, 1991, 30, 34.

[3] Special issue on polyoxometalates: ed. C. Hill, *Chem. Rev.*, 1998, **98**.

[4] T. Yamase, *Chem. Rev.*, 1998, **98**, 307.

[5] I. Moriguchi, J. H. Fendler, *Chem. Mater.*, 1998, 10, 2205.

[6] S. Q. Liu, D. G. Kurth, H. Möhwald and D. Volkmer, *Adv. Mater.*, 2002, **14**, 225.

[7] C.L. Hill, D.A. Bouchard, M. Kadkhodayan, M. Williamson, J. A. Schmidt and E. F. Hilinski, J. Am. Chem. Soc., 1988, **110**, 5471.

[8] G. R. Pedro and L. C. Morica, *Adv. Mater.*, 1997, **9**, 144.

[9] P. Maguerès, S. M. Hubig, S. V. Lindeman, P. Veya and J. K. Kochi, *J. Am. Chem. Soc.*, 2000, **122**, 10073.

[10] G. Zhang, W. Yang and J. Yao, *Adv. Funct. Mater.*, 2005, 15, 1255.

[11] S. Liu, H. Möhwald, D. Volkmer and D. G. Kurth, *Langmuir*, 2006, **22**, 1949.

[12] J. Lu, E. Shen, M. Yuan, Y. Li, E. Wang, C. Hu, L. Xu and J. Peng, *Inorg. Chem.*, 2003, **42**, 6956.

[13] V. Shivaiah, M. Nagaraju and S. K. Das, *Inorg. Chem.*, 2003, **42**, 6604.

[14] H. An, Y. Li, E. Wang, D. Xiao, C. Sun, L. Xu, Inorg. Chem., 2005, **44**, 6062.

[15] C. -M. Liu, D. -Q. Zhang, M. Xiong and D. -B. Zhu, *Chem. Commun.*, 2002, 1416.

[16] J. Lu, Y. Xu, N. K. Goh and L. S. Chia, *Chem. Commun.*, 1998, 2733.

[17] P. -Q. Zheng, Y. -P. Ren, L. -S. Long, R. -B. Huang and L. -S. Zheng, *Inorg. Chem.*, 2005, **44**, 1190.

[18] M. I. Khan, E. Yohannes and D. Powell, *Chem. Commun.*, 1999, 23.

[19] M. I. Khan, E. Yohannes and R. J. Doedens, *Angew. Chem., Int. Ed.*, 1999, **38**, 1292.

[20] S. -T. Zheng, J. Zhang and G. -Y. Yang, *Inorg. Chem.*, 2005, **44**, 2426.

[21] A. Dolbecq, P. Mialane, L. Lisnard, J. Marrot and F. Sécheresse, *Chem. −Eur. J.*, 2003, **9**, 2914.

[22] J. Lu, E. Shen, Y. Li, D. Xiao, E. Wang and L. Xu, *Cryst. Growth Des.*, 2005, **5**, 65.

[23] H. Zhang, L. Duan, Y. Lan, E. Wang and C. Hu, *Inorg. Chem.*, 2003, **42**, 8053.

[24] I. A. Kahwa, J. Selbin, C. J. Oconnor, J. W. Foise and G. L. McPherson, *Inorg. Chim. Acta*, 1988, 148, 265.

[25] Z. He, E. -Q. Gao, Z. -M. Wang, C. -H. Yan and M. Kurmoo, *Inorg. Chem.*, 2005, **44**, 862.

[26] G. Vicentini, L. B. Zinner, J. Zukerman-Schpector, K. Zinner, *Coord. Chem. Rev.*, 2000, **196**, 353.

[27] A. Patra, C. S. Friend, R. Kapoor and P. N. Prasad, *J. Phys. Chem. B*, 2002, **106**, 1909.

3.2 Solid-State Photopolymerization of $[Gd_2(NMP)_{12}(PW_{12}O_{40})][PW_{12}O_{40}]$

3.2.1 Introduction

Photochromic compounds are subjects of growing interest because of their potential technological applications in the areas of information display devices, solar energy conversion, high-density memory devices, and photoelectric sensors [1]. It is well-known that one of the most important properties of polyoxometalates is the capability to accept various numbers of electrons giving rise to mixed-valency colored species (heteropolyblues or heteropolybrowns) [2], which make them suitable for photochromic and electrochromic materials [2–4]. Since the investigation of inorganic-organic hybrid materials became an expanding field, the preparation, microstructure, and photochromic process of polyoxometalates-based hybrid composites have been extensively investigated [5].

On the other hand, despite the inherent strong barriers of simultaneous bond breaking and formation in more than one direction, single-crystal-to-single-crystal (SCSC) transformations in the solid state have been studied widely in recent years [6, 7]. However, much of the work has focused on thermal-stimulated [6] or guest desorption/absorption-induced [7] types, while the photo-induced type received less attention. Herein, we report an interesting discovery of a photo-polymerized SCSC transformation in a photochromic polyoxometalates-based hybrid, $[Gd_2(NMP)_{12}(PW_{12}O_{40})][PW_{12}O_{40}]$ (NMP = *N*-methyl-2-pyrrolidone) (**1**), in which reversible photochromism occurred with reversible structural transformation under irradiation with sunlight.

3.2.2 Results and discussion

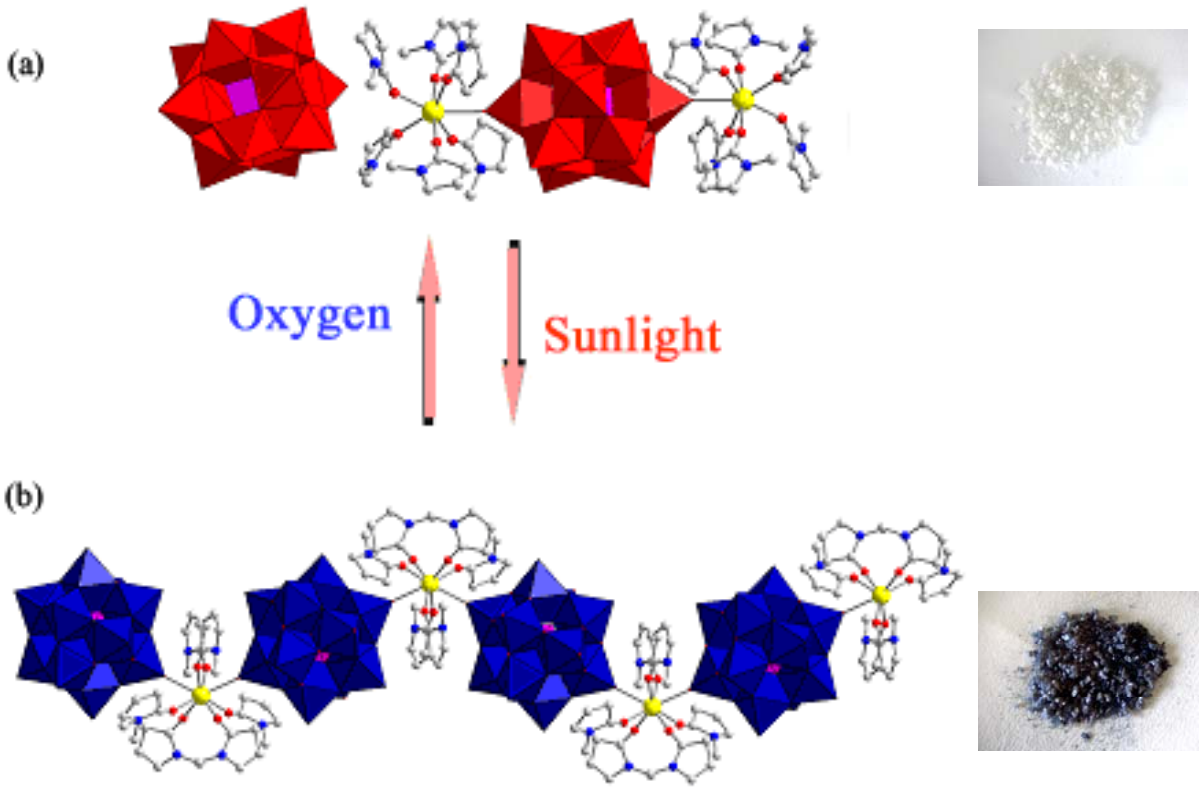

Fig. 1 Process of photochromism and SCSC transformation. a) Ball and stick and polyhedral representations of **1**. The color code is as follows: Gd (yellow), O (red), N (blue), C (gray), WO_6 (red), PO_4 (purple); b) Ball and stick and polyhedral representations of **2**. The color code is as follows: Gd (yellow), O (red), N (blue), C (gray), WO_6 (deep-blue), PO_4 (purple).

Reaction of $GdCl_3$, $H_3PW_{12}O_{40}$ and NMP in CH_3CN/H_2O (2:1, v/v) followed by slow evaporation at room temperature in the black position resulted in colorless single crystals‡. X-ray analyses‡ reveal that compound **1**, belonging to the triclinic system, exhibits an ionic, asymmetric structure consisting of the $[PW_{12}O_{40}]^{3-}$ anion and the $[Gd_2(NMP)_{12}(PW_{12}O_{40})]^{3+}$ cation in which either of Gd^{III} ions is coordinated with 6 NMP molecules and connected by $[PW_{12}O_{40}]^{3-}$ (Fig. 1a). The coordination polyhedron of Gd^{III} may be represented as a highly distorted, single-capped trigonal prism (Fig. 3a). The Gd-O bond lengths are within the range from 2.212 to 2.514 Å (mean value 2.316 Å). The torsion angle between the top plane and the bottom plane is 27.89 °.

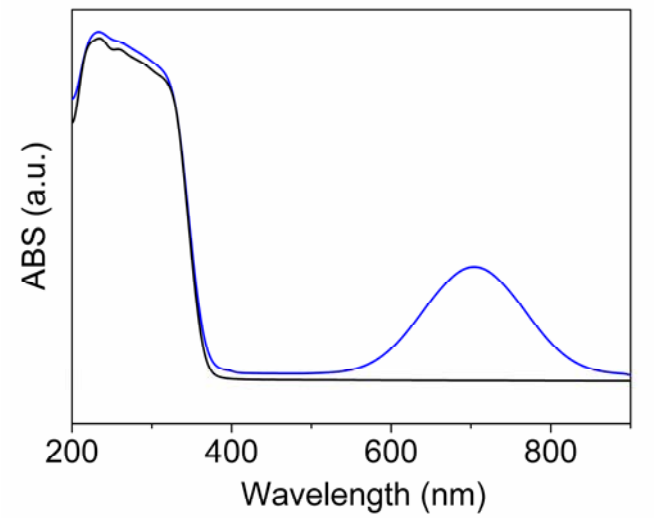

Fig. 2 The solid-state UV-vis spectra before (black curve) and after (blue curve) irradiation with sunlight.

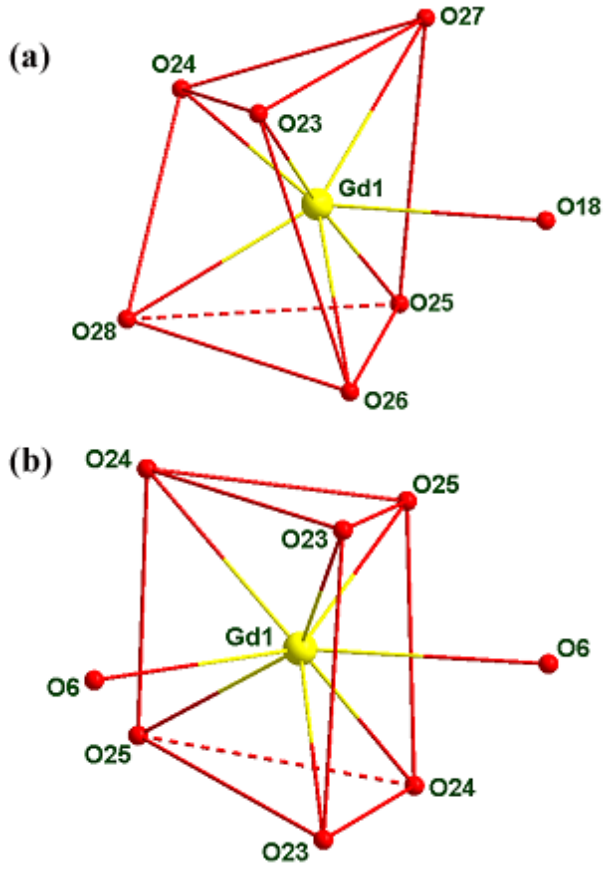

Fig. 3 a) Coordination polyhedron around Gd^{III} in **1**; b) Coordination polyhedron around Gd^{III} in **2**.

When exposed to sunlight, colorless crystals of **1** turn deep blue gradually. This observation should be attributed to the electron transfer between electron donors of organic molecules and electron acceptors of polyoxometalate anions. The final result is that W^{VI} atoms of the polyanions are reduced and mixed-valence compounds are formed, leading to the observed photochromism [2]. UV-vis spectra (Fig. 2) indicated that, after irradiation with sunlight, the absorption band at 700 nm in visible region appeared due to metal-to-metal extra intervalence charge transfer (IVCT) ($W^{5+} \rightarrow W^{6+}$) [8]. Compared with those well-reported discrete charger-transfer alkylammonium-polyoxometalates [2], the speculated photochromic mechanism of **1** is slightly different. A reasonable mechanism should involve the absorption of photons by the Keggin structure, resulting in the generation of an electron-hole pair which directly oxidizes NMP into NMP^{+} through O−Gd−O not the hydrogen bond.

When we performed the X-ray analyses on the resulted deep blue crystals, unexpectedly, structural transformation occurred in the photochromic hybrid and a new compound belonging to monoclinic system, $[Gd(NMP)_6(PW_{12}O_{40})]_n$ (**2**), was obtained.‡ Compound **2** consists of a 1-D infinite zigzag chain built from alternate polyanions and $[Gd(NMP)_6]^{3+}$ subunits and displays a $\{(anion)M\text{-}donor\}_n$ (M = Gd; anion = $PW_{12}O_{40}^{3-}$; donor = NMP) type of structure (Fig. 1b). The coordination polyhedron of Gd^{III} may be represented as a distorted, bicapped trigonal prism (Fig. 3b). The Gd−O bond lengths are within the range from 2.255 to 2.526 Å (mean value 2.359 Å). The torsion angle between the top plane and the bottom plane is 7.29 °, which is smaller than that of compound **1** (Δ = 20.60 °).

To further contrast **1** with **2**, in the packing framework of **1**, we can find a discontinuous zigzag chain (Fig. 4). The distance of adjacent polyanions is 137.77 Å (defined by the P···P separation), which is equal to that in the continuous zigzag chain of

2. The turning angle of P···Gd···P (104.73°) in **1** is slightly smaller than that (125.81°) in **2** (Δ = 21.08 °; the difference is almost equal to that in the torsion angle of Gd^{III} coordination polyhedrons). In addition, the NMP ligands in both **1** and **2** are highly disordered. These structural values and factors provide a potential environment for the SCSC transformation. To further examine the phase purity of this system, X-ray powder diffraction was carried out on **1** and **2**, respectively (Fig. 5). The comparison between the experimental pattern and the calculated pattern (based on single-crystal data) shows that both **1** and **2** are pure. When the crystals of **2** are placed in the air and sheltered from the light, they gradually turn back to their original colorlessness. X-ray analyses reveal that with the color changes compound **2** simultaneously converts 1-D zigzag chains into original zero-D ionic structures. If color-changed samples are put under nitrogen atmosphere and sheltered from the light, their color does not fade, indicating that the fading process is a chemical one and that it is the oxygen in the air that has reoxidized W^{V} into W^{VI}, not the self-redox occurring in the system. The whole process might concisely proceed in Fig. 1. Also deserving attention, by heating at 90 °C in air under sunlight, the color and structural reversal also occur in compound **2**, which indicates that the reverse SCSC transformation of **2** to **1** can be also considered as a thermal-stimulated type; however, nothing occurs when heating is carried out in nitrogen atmosphere, which further indicates that reverse transformation of **2** to **1** is significantly affected by oxygen.

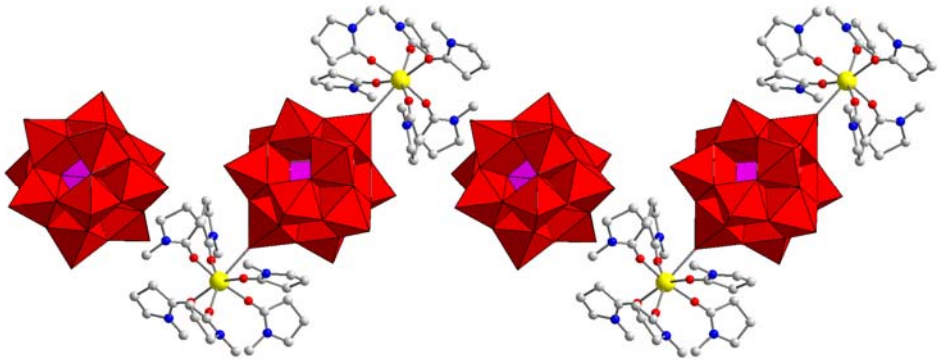

Fig. 4 A discontinuous zigzag chain existing in the packing structures of **1**.

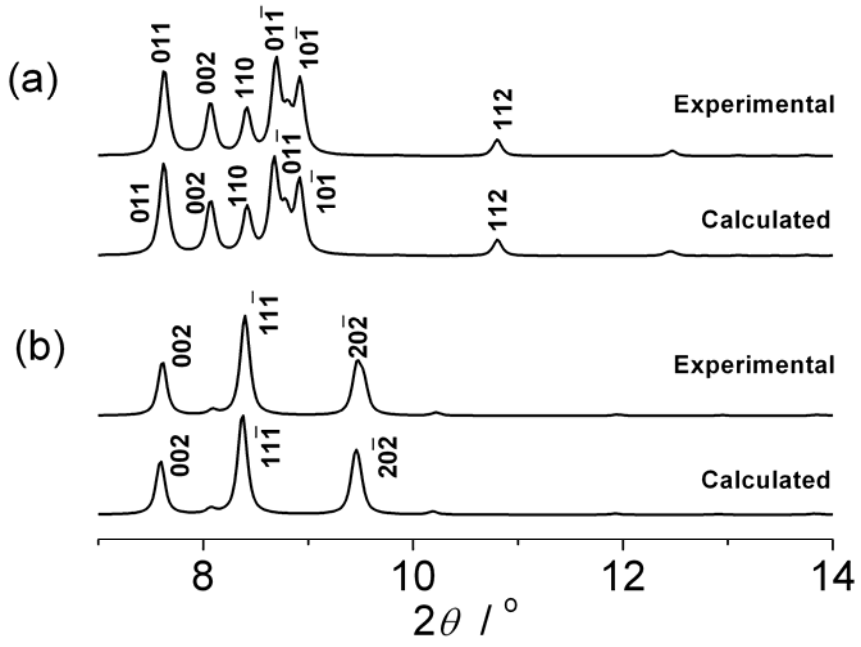

Fig. 5 XRPD patterns of a) **1** and b) **2**. The figures showed the Miller indices of each reflection (2θ < 14°).

To further explore this phenomenon, it is interesting to compare compounds **1** and **2** with analogous compounds reported in **Section 3.1**, $[Pr(NMP)_6(PW_{12}O_{40})]_n$, $[Eu(NMP)_6(PW_{12}O_{40})]_n$ and $[Er_2(NMP)_{12}(PW_{12}O_{40})][PW_{12}O_{40}]$. The structures of **Pr** and **Eu** are isomorphous to **2** while the structure of **Er** is isomorphous to **1**. From 1-D chains of

compounds **Pr** and **Eu** to zero-D ionic frameworks of compounds **1** and **Er**, these structural changes illustrate the Gd may be the turning point from zero-D to 1-D structure in the series of lanthanides compounds because of lanthanide contraction. Similar to **1**, compounds **Pr**, **Eu** and **Er** are all photochromic. However when the similar experiments of X-ray analyses were carried on the three compounds, photo-induced structural transformation never occurred in them but only occurred in compound **1**. According to the above results, the photo-induced SCSC transformation might be connected with the turning point.

3.2.3 Summary

In summary, a photochromic 12-tungstophosphate-based hybrid has been synthesized, in which a reversible photopolymerization interestingly occurred. To the best of our knowledge, this Communication provides the first polyoxometalates-based example of SCSC transformations. Furthermore, it is highly interesting to study the photomagnetism, electrochemistry, and photoelectricity in the system, because there is not only SCSC transformation but also deoxidized W^{V} atoms under irradiation with sunlight.

References

‡ Synthesis of compound **1**: An aqueous solution (10 mL) containing $H_3PW_{12}O_{40}{\cdot}nH_2O$ (1.3 g) and $GdCl_3{\cdot}6H_2O$ (0.1487 g, 0.4 mmol) was heated to dryness at 90 °C in a water bath. *N*-methyl-2-pyrrolidone (0.5 mL) was then added into the resultant dry solid with stirring until the mixture became a paste. Finally, the paste was dissolved in an acetonitrile/water (2:1, v/v) mixed solution (10 mL), filtered and left standing to concentrated at room temperature in the dark. After a few days, colorless crystals suitable for X-ray analyses were obtained (1.16 g, yield 80 %). Anal. Calcd (%) for **1**: C 9.9, H 1.5, N 2.3; Found: C 10.1, H 1.7, N 2.2. IR (KBr, *v*): 3405 (s), 2937 (w), 1641(vs), 1513 (m), 1407 (w), 1308 (w), 1260 (w), 1259 (m), 1082 (vs), 984 (vs), 895 (vs), 814 (vs), 523(m) cm^{-1}. UV-vis (solid-state, λ_{max}): 250 nm. Crystal data of **1**: $C_{60}H_{108}N_{12}O_{92}P_2Gd_2W_{24}$, M_r = 7258.42, triclinic, $P\bar{1}$, a = 12.119(2) Å, b = 13.598(3) Å, c = 22.210(4) Å, α = 80.328(3)° , β = 85.395(3)°, γ = 67.725(3)°, V = 3338.3(11) $Å^3$, Z = 1, ρ_{calcd} = 3.610 g cm^{-3}, $2\theta_{max}$ =

50.04° ($-14 \leq h \leq 14$, $-16 \leq k \leq 11$, $-26 \leq l \leq 26$), T = 294(2) K, $F(000)$ = 3222, GOF = 1.054, R_1 = 0.0536, wR_2 = 0.1135. CCDC−611433.

Synthesis of compound **2**: When exposed to sunlight for 5 h, crystals of **1** completely turned deep blue and produced compound **2**. Anal. Calcd (%) for **2**: C 9.9, H 1.5, N 2.3; Found: C 10.2, H 1.6, N 2.3. IR (KBr, *v*): 3403 (s), 2932 (w), 1639 (vs), 1514 (m), 1408 (w), 1309 (w), 1260 (w), 1259 (m), 1081 (vs), 985 (vs), 899 (vs), 809 (vs), 522 (m) cm^{-1}. UV-vis (solid-state, λ_{max}): 250, 700 nm. Crystal data of **2**: $C_{30}H_{54}N_6O_{46}PGdW_{12}$, M_r = 3629.21, monoclinic, *C*2/c, a = 22.058(7) Å, b = 12.811(7) Å, c = 24.390(9) Å, α = 90° , β = 107.460(6)°, γ = 90°, V = 6574(5) $Å^3$, Z = 4, ρ_{calcd} = 3.667 g cm^{-3}, $2\theta_{max}$ = 50.02° ($-26 \leq h \leq 23$, $-11 \leq k \leq 15$, $-26 \leq l \leq 29$), T = 294(2) K, $F(000)$ = 6444, GOF = 1.142, R_1 = 0.0523, wR_2 = 0.1245. CCDC−633062.

[1] (a) G. H. Brown, *Photochromism*, Wiley, New York, 1971; (b) J. N. Yao, K. Kashimoto and A. Fujishima, *Nature*, 1992, **355**, 624; (c) J. N. Yao, P. Chen and A. Fujishima, *J. Electroanal. Chem.*, 1996, **406**, 223; (d) S. Nagashima, M. Murata and H. Nishihara, *Angew. Chem., Int. Ed.*, 2006, **45**, 4298; (e) M. Bossi, V. Belov, S. Polyakova and S. W. Hell, *Angew. Chem., Int. Ed.*, 2006, **45**, 7462.

[2] T. Yamase, *Chem. Rev.* 1998, **98**, 307.

[3] I. Moriguchi and J. H. Fendler, *Chem. Mater.*, 1998, **10**, 2205.

[4] S. Q. Liu, D. G. Kurth, H. Möhwald and D. Volkmer, *Adv. Mater.*, 2002, **14**, 225.

[5] (a) C. L. Hill, D. A. Bouchard, M. Kadkhodayan and M. Williamson, J. A. Schmidt, E. F. Hilinski, *J. Am. Chem. Soc.*, 1988, **110**, 5471; (b) G. R. Pedro and L. C. Morica, *Adv. Mater.*, 1997, **9**, 144; (c) P. Maguerès, S. M. Hubig, S. V. Lindeman and P. Veya, J. K. Kochi, *J. Am. Chem. Soc.*, 2000, **122**, 10073; (d) G. Zhang, W. Yang and J. Yao, *Adv. Funct. Mater.*, 2005, **15**, 1255; (e) S. Liu, H. Möhwald, D. Volkmer and D. G. Kurth, *Langmuir*, 2006**, 22**, 1949.

[6] (a) C. Hu and U. Englert, *Angew. Chem., Int. Ed.*, 2005, **44**, 2281; (b) J. -P. Ma, Y. -B. Dong, R. -Q. Huang, M. D. Smith and C. -Y. Su, *Inorg. Chem.*, 2005, **44**, 6143; (c) J. -P. Zhang, Y. -Y. Lin, W. -X. Zhang and X. M. Chen, *J. Am. Chem. Soc.*, 2005, **127**, 14162. (d) J. D. Ranford, J. J. Vittal, D. Wu, *Angew. Chem., Int. Ed.*, 1998, **37**, 1114; (e) J. D. Ranford, J. J. Vittal and D. Wu, X. Yang, *Angew.Chem., Int. Ed.*, 1999, **38**, 3498.

[7] (a) C. -L. Chen, A. M. Goforth, M. D. Smith, C. -Y. Su and H. -C. zur Loye, *Angew. Chem., Int. Ed.*, 2005, **44**, 6673; (b) G. J. Halder and C. J. Kepert, *J. Am. Chem. Soc.*, 2005, **127**, 7891; (c) K. Takaoka, M. Kawano, M. Tominaga and M. Fujita, *Angew. Chem., Int. Ed.*, 2005, **44**, 2151; (d) O. Ohmori, M. Kawano and M. Fujita, *J. Am. Chem. Soc.*, 2004, **126**, 16292; (e) S. Kitagawa and K. Uemura, *Chem. Soc. Rev.*, 2005, **34**, 109; (f) C. -D. Wu and W. Lin, *Angew. Chem., Int. Ed.*, 2005, **44**, 1958; (g) M. Nihei, L. Han and H. Oshio, *J. Am. Chem. Soc.*, 2007, **129**, 5312.

[8] M. T. Pope, *Heteropoly and Isopoly Oxometalates*, Springer-Verlag, Berlin, 1983.

Chapter 4 Hydrophilic compounds built on Anderson POMs

4.1 Introduction

It is well known that many materials can undergo solid-state structural phase transformation as a function of temperature, and that different atomic arrangements are stable in different temperature ranges [1]. With development of crystal engineering, temperature-dependent single-crystal-to-single-crystal (SCSC) phase transformations have received considerable interest [2−5]. However, such SCSC phase transformations are still rare since crystals can hardly retain single crystallinity after the solid-state rearrangement of atoms.

Polyoxometalates (POMs) are nano-sized metal-oxygen cluster species with a diverse compositional range and an enormous structural variety [6−11]. One of the most important properties of polyoxometalates is the capability to accept large and various numbers of water molecules in their crystal lattice, which make them very useful in the hydration catalysis [6, 11]. Since it has been demonstrated that water molecules can play an important role in SCSC phase transformations as a function of temperature [12], polyoxometalates can be good candidates for investigation into temperature-dependent SCSC phase transformations. However, to the best of our knowledge, the temperature-dependent SCSC phase transformation of polyoxometalates has been unknown in the literature.

Herein, we construct the simple but highly hydrophilic polyoxometalate $[Tm_2(H_2O)_{14}CrMo_6O_{24}H_6][CrMo_6O_{24}H_6]\cdot 16\ H_2O$ by using the Anderson-type anion and the lanthanide cation, and report the temperature-dependent SCSC phase transformation that occurs at surprisingly low temperature (< 113 K).

4.2 Results and discussion

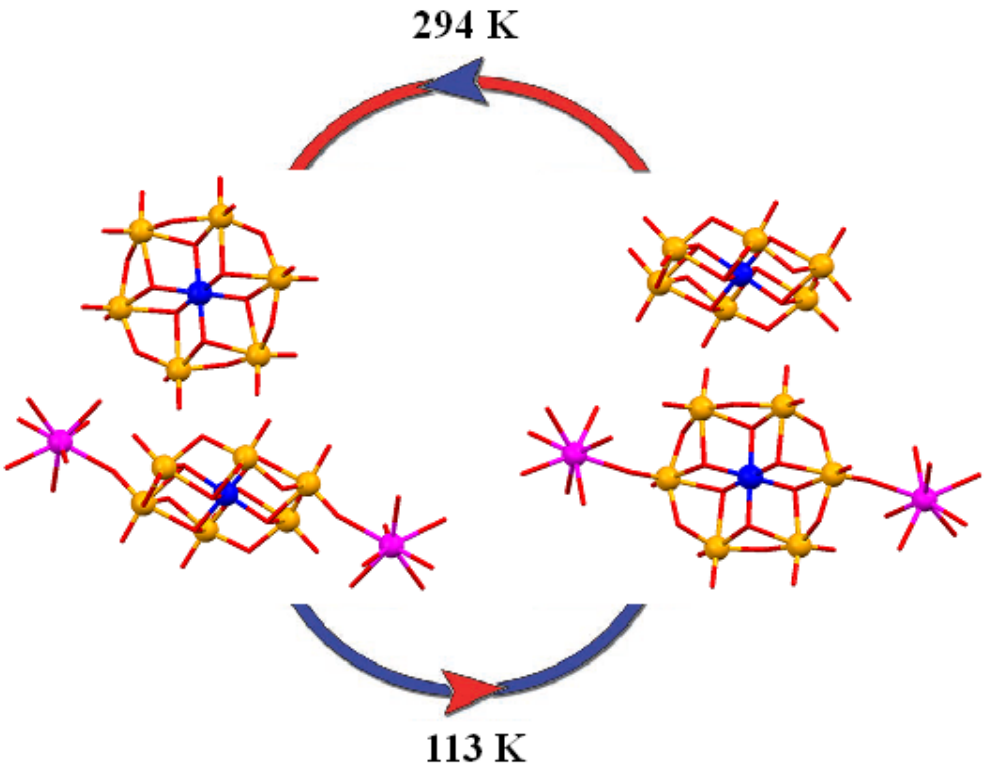

Fig. 1 Process of the temperature-induced SCSC transformation. left) Ball and stick representations of **1**; right) Ball and stick representations of **1′**. The color code is as follows: thulium (purple), molybdenum (yellow), chromium (blue), and oxygen (red).

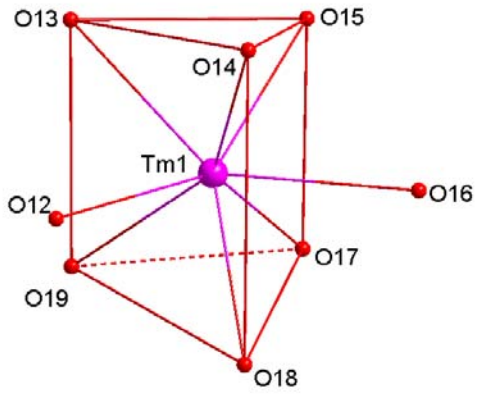

Fig. 2 Coordination polyhedron around Tm in **1**. Bond lengths (Å): Tm(1)−O(12), 2.390(5); Tm(1)−O(13), 2.377(5); Tm(1)−O(14), 2.293(6); Tm(1)−O(15), 2.317(8); Tm(1)−O(16), 2.386(6); Tm(1)−O(17), 2.327(6); Tm(1)−O(18), 2.301(6); Tm(1)−O(19), 2.294(6).

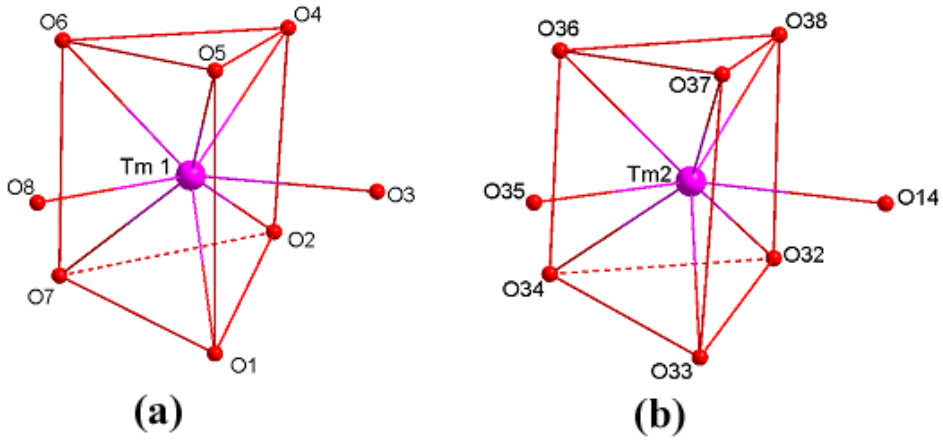

Fig. 3 Coordination polyhedron around (a) Tm1 and (b) Tm2 in **1′**. Bond lengths (Å): Tm(1)−O(1), 2.282(5); Tm(1)−O(2), 2.330(6); Tm(1)−O(3), 2.360(6); Tm(1)−O(4), 2.357(5); Tm(1)−O(5), 2.309(5); Tm(1)−O(6), 2.330(6); Tm(1)−O(7), 2.384(5); Tm(1)−O(8), 2.387(6); Tm(2)−O(14), 2.407(6); Tm(2)−O(32), 2.382(5); Tm(2)−O(33), 2.340(6); Tm(2)−O(34), 2.316(5); Tm(2)−O(35), 2.429(5); Tm(2)−O(36), 2.310(5); Tm(2)−O(37), 2.287(5); Tm(2) −O(38), 2.272(6).

Reaction of $TmCl_3 \cdot 6H_2O$ (0.2 mmol, 0.055 g) and $Na_3[CrMo_6O_{24}H_6] \cdot 8H_2O$ (0.2 mmol, 0.25 g) [13] in an aqueous solution (10 mL) at 80 °C for 1 h followed by slow evaporation at room temperature resulted in pink single crystals (0.14 g, yield 48 %) [14]. X-ray analyses at 294 K reveal that the compound, crystallized as $[Tm_2(H_2O)_{14}CrMo_6O_{24}H_6][CrMo_6O_{24}H_6] \cdot 16H_2O$ (**1**), belongs to triclinic $P\bar{1}$ space group with the lattice parameters of a = 11.0989(13), b = 11.7203(14), c = 13.9843(16) Å; α = 74.993(2), β = 84.548(2), γ = 89.545(2)° [15]. **1** exhibits an ionic, asymmetric structure consisting of the $[CrMo_6O_{24}H_6]^{3-}$ polyoxoanion and the $[Tm_2(H_2O)_{14}CrMo_6O_{24}H_6]^{3+}$ polyoxocation (Fig. 1). In this structure, the two Cr atoms lie on independent inversion centres and as a consequence the asymmetric unit has one Tm-containing moiety in a general position and two half Cr-containing moieties. In the polyoxocation, either of Tm^{III} ions is coordinated with 7 water molecules and is bound to the Anderson core by one oxygen atom. The coordination polyhedron of Tm^{III} can be represented as a distorted,

bicapped trigonal prism (Fig. 2). The Tm−O bond lengths are within the range from 2.293 to 2.390 Å (mean value 2.336 Å). The torsion angle between the top plane and the bottom plane is 18.92°. The distance of strictly symmetrical Tm^{III} ions (Tm···Tm) is 13.768 Å. The angle of Tm···Cr···Tm is 180°, showing the three atoms are strictly linear. The distance between the polyoxocation and the polyoxoanion is 8.039 Å (defined by the Cr···Cr separation).

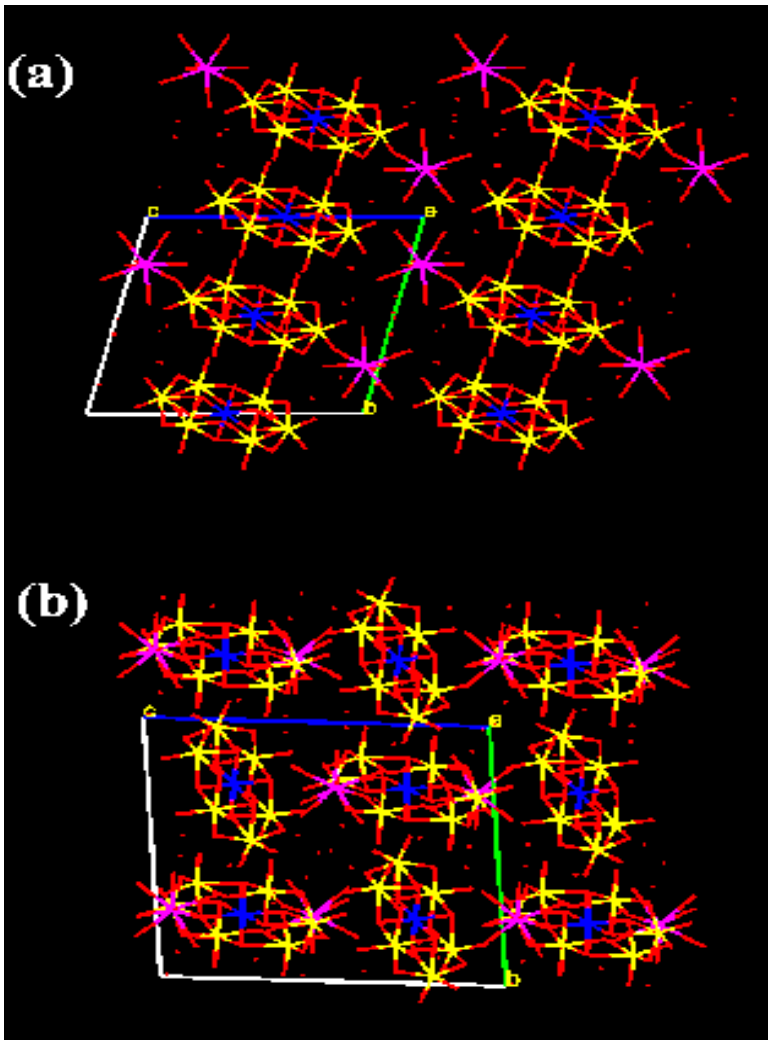

Fig. 4 View of three-dimensional structures running to the *a* axis for (a) **1** and (b) **1′**.

In the X-ray analyses, when the crystal of **1** was cooled from 294 K to temperatures below ca. 113 K, the change in lattice parameters was observed. Phase **1′**, crystallized as

$[Tm_2(H_2O)_{14}CrMo_6O_{24}H_6][CrMo_6O_{24}H_6]\cdot 16H_2O$, belongs to triclinic $P\bar{1}$ space group with the lattice parameters of a = 15.607(4), b = 15.934(5), c = 16.088(5) Å; α = 86.667(12), β = 72.242(9), γ = 64.394(9)° [16]. **1′** exhibits a very similar ionic, asymmetric structure to **1**, consisting of the $[CrMo_6O_{24}H_6]^{3-}$ polyoxoanion and the $[Tm_2(H_2O)_{14}CrMo_6O_{24}H_6]^{3+}$ polyoxocation with the distance of 8.040 Å (Fig. 1). However, unlike that of **1**, in this structure, the asymmetric unit has the two Tm-containing and two Cr-containing moieties all in general positions. In the polyoxocation of **1′**, two Tm^{III} ions are not strictly symmetrical. The Tm−O bond lengths of the two Tm^{III} ions are within the range from 2.282 to 2.387 Å (mean value 2.342 Å) and from 2.272 to 2.429 Å (mean value 2.343 Å), respectively. The torsion angles between the top plane and the bottom plane in their distorted, bicapped trigonal prisms (Fig. 3) are 19.05° and 15.38°, respectively. The arrangement of Tm···Cr···Tm (strictly linear in **1**) is slightly distorted with the angle 178.20°. By comparison of the ionic structures shown in Fig. 1 and the packing frameworks shown in Fig. 4, the significant difference between **1** and **1′** was found as the relative conformation of polyoxocations ($[Tm_2(H_2O)_{14}CrMo_6O_{24}H_6]^{3+}$) and polyoxoanions ($[CrMo_6O_{24}H_6]^{3-}$), which resulted in the final phase transformation. X-ray analyses of different single crystals of **1** at 113 K indicated that the phase **1′** could be quickly detected. When **1′** was warmed above 113 K, it quickly transformed back to **1**. The results further demonstrate that the transformation between phase **1** and phase **1′** was fast and reversible. Although the phase transformation can be directly observed by the changes of lattice parameters and packing frameworks, it is difficult to explain the detailed mechanism because the guest water molecules are all disordered and the hydrogen bonds in this system are very complex (Fig. 5). We can speculate that there should be cooperative movement between clusters and guest water

molecules in the crystal lattice. It would be a challenge to study the mechanism of temperature-dependent SCSC phase transformations in polyoxometalates systems.

To examine the thermal stability of compound **1**, thermal gravimetric analysis (TGA) was carried out in the range of 25−900 °C (Fig. 6). Crystalline samples collapsed from 40 °C, indicating that polyoxometalates are not suitable for calefactive investigation into SCSC phase transformations. There were two major water-loss steps. The first step between 40 and 170 °C by the weight loss of 10.11 %, corresponded to the loss of all uncoordinated water molecules (calcd 9.88 % for $16H_2O$). At the second step, the compound lost coordinated water molecules (the weight loss of 8.95 %) between 170 and 300 °C (calcd 8.65 % for $14H_2O$) but did not decompose until 700 °C. Our preliminary data indicate that compound **1** can undergo a few desorption and adsorption cycles. When the resulted sample at the second step was exposed to atmospheric humidity at room temperature overnight, water was readsorbed, as shown by the recovery of the 17.48 % weight loss below 300 °C upon a second thermal treatment (Fig. 7). Interestingly, rehydration did not render the sample amorphous and a clear XRD pattern was observed (Fig. 8a). The XRD comparison (Fig. 8) showed that the original ionic hydration structure was potentially recovered on rehydration (with some loss of crystallinity). It appears that the water is necessary to hold the clusters in place and maintain the stability of the whole compound. These results indicate that this adsorption system may provide some reversible coordination bonds and hydrogen bonds. The sorption feature is slightly different from that in those well-reported porous metal-organic frameworks [17], in which adsorption properties are connected with holes or channels.

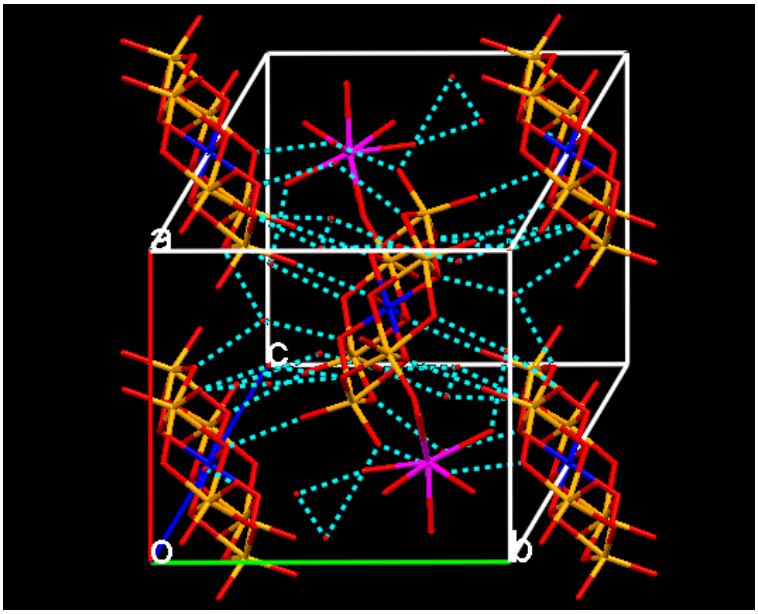

(a)

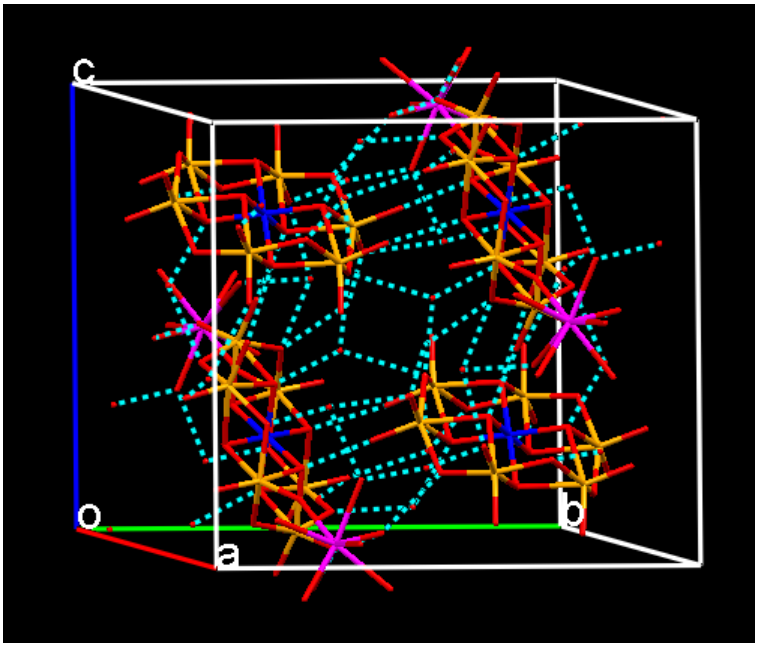

(b)

Fig. 5 View of complex hydrogen bonds for (a) phase **1** and (b) phase **1′**.

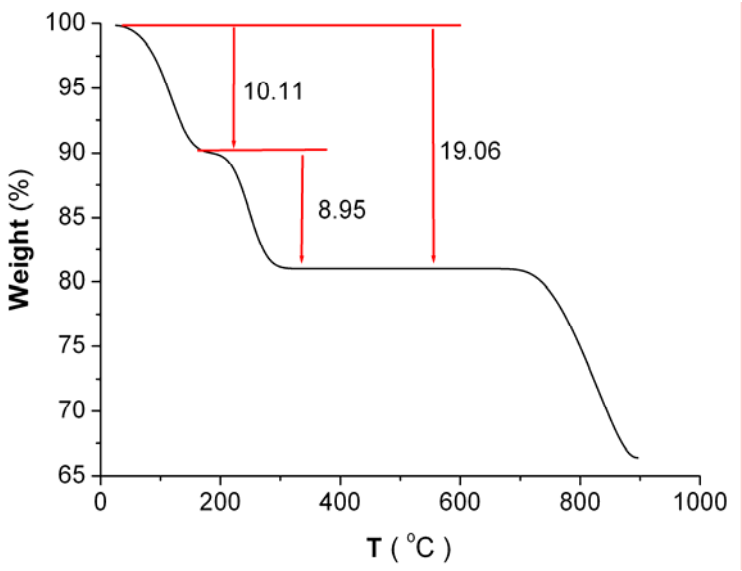

Fig. 6 Thermal gravimetric analysis data of **1**.

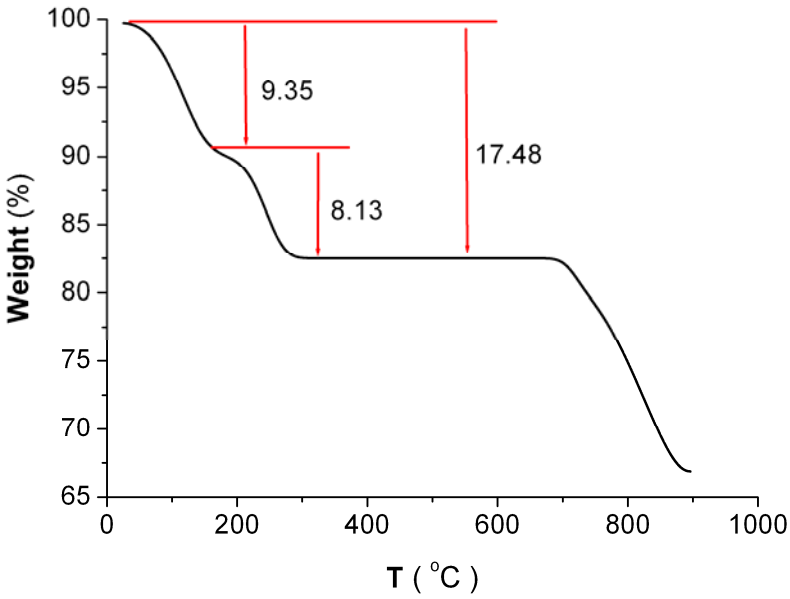

Fig. 7 Thermal gravimetric analysis data of **1** upon a second thermal treatment.

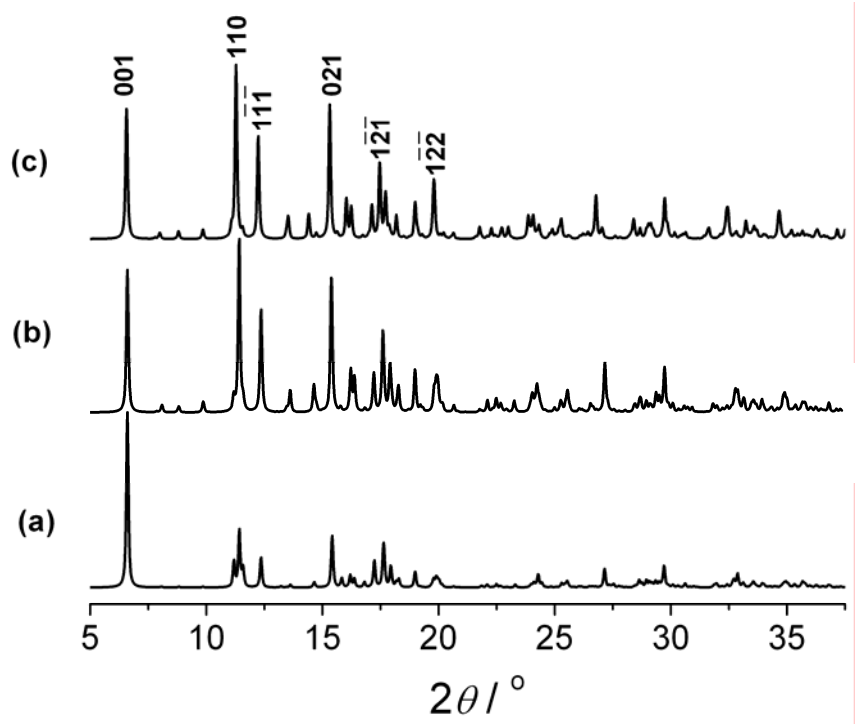

Fig. 8 XRD patterns of (a) rehydrated samples, (b) original crystalline samples and (c) calculated results from the single-crystal data of **1**.

4.3 Summary

In conclusion, the rare-earth Anderson-type polyoxometalate $[Tm_2(H_2O)_{14}CrMo_6O_{24}H_6][CrMo_6O_{24}H_6]\cdot 16\ H_2O$ undergoes the single-crystal-to-single-crystal phase transformation at low temperature. The results indicate that polyoxometalates can be good candidates for investigation into temperature-dependent SCSC phase transformations. We expect that this example can provide some useful information for the studies of SCSC phase transformations of polyoxometalates.

References

[1] E. C. Aifantis and J. Gittus, *Phase Transformations*, Elsevier, London, 1986.

[2] C. Hu and U. Englert, *Angew. Chem., Int. Ed.*, 2005, **44**, 2281.

[3] J. -P. Ma, Y. -B. Dong, R. -Q. Huang, M. D. Smith and C. -Y. Su, *Inorg. Chem.*, 2005, **44**, 6143.

[4] M. R. Caira, L. R. Nassimbeni, H. Su and E. Weber, *CrystEngComm*, 2003, **5**, 351.

[5] E. C. Spencer, J. A. K. Howard, P. K. Baruah and G. J. Sanjayan, *CrystEngComm*, 2006, **8**, 469.

[6] M. T. Pope, *Heteropoly and Isopoly Oxometalates*, Springer-Verlag, Berlin, 1983.

[7] *Polyoxometalates: From Platonic Solids to Anti-Retroviral Activity*, ed. M. T. Pope and A. Müller, Kluwer, Dordrecht, The Netherlands, 1994.

[8] *Polyoxometalate Chemistry: From Topology via Self-Assembly to Applications*, ed. M. T. Pope and A. Müller, Kluwer, Dordrecht, The Netherlands, 2001.

[9] *Polyoxometalate Chemistry for Nano-Composite Design*, ed. T. Yamase and M. T. Pope, Kluwer, Dordrecht, The Netherlands, 2002.

[10] M. T. Pope and A. Müller, *Angew. Chem., Int. Ed.*, 1991, **30**, 34.

[11] Special issue on polyoxometalates: ed. C. Hill, *Chem. Rev.*, 1998, **98**.

[12] C. Janiak and T. G. Scharmann, *J. Am. Chem. Soc*., 2002, **124**, 14010.

[13] A. Perloff, *Inorg. Chem.*, 1970, **9**, 2228.

[14] Anal. Calcd (Found) (%): Cr 3.6 (3.4), Mo 39.5 (39.2), Tm 11.6 (11.3). FT-IR (cm^{-1}): 3340 (s), 951 (s), 904 (vs), 840 (w), 757 (m), 642 (vs), 532 (m), 422 (m). UV-vis (solid-state, nm): 260, 390, 523.

[15] Crystal data for **1**: $H_{72}Cr_2Mo_{12}O_{78}Tm_2$, M_r = 2913.72, triclinic, $P\bar{1}$, a = 11.0989(13) Å, b = 11.7203(14) Å, c = 13.9843(16) Å, α = 74.993(2)° , β = 84.548(2)°, γ = 89.545(2)°, V = 1748.9(4) $Å^3$, Z = 1, ρ_{calcd} = 2.767 g cm^{-3}, $2\theta_{max}$ = 52.84° ($-9 \le h \le 13$, $-12 \le k \le 14$, $-15 \le l \le 17$), T = 294(2) K, F(000) = 1386, 36 restraints used in the refinement, GOF = 1.012, R_1 = 0.0476, wR_2 = 0.1339. CSD no. 417007.

[16] Crystal data for **1′**: $H_{72}Cr_2Mo_{12}O_{78}Tm_2$, M_r = 2913.72, triclinic, $P\bar{1}$, a = 15.607(4) Å, b = 15.934(5) Å, c = 16.088(5) Å, α = 86.667(12)° , β = 72.242(9)°, γ = 64.394(9)°, V = 3423.3(17) $Å^3$, Z = 2, ρ_{calcd} = 2.827 g cm^{-3}, $2\theta_{max}$ = 55.80° ($-20 \le h \le 20$, $-19 \le k \le 20$, $-19 \le l \le 21$), T = 113(2) K, F(000) = 2772, 162 restraints used in the refinement, GOF = 1.065, R_1 = 0.0434, wR_2 = 0.1265. CSD no. 417560.

[17] (a) S. Kitagawa, R. Kitaura and S. Noro, *Angew. Chem., Int. Ed.*, 2004, **43**, 2334; (b) A. K. Cheetham, G. Férey and T. Loiseau, *Angew. Chem., Int. Ed.*, 1999, **38**, 3268; (c) S. Uchida and N. Mizuno, *J. Am. Chem. Soc.*, 2004, **126**, 1602; (d) R. Kawamoto, S. Uchida and N. Mizuno, *J. Am. Chem. Soc.*,

2005, **127**, 10560; (e) K. Uehara, H. Nakao, R. Kawamoto, S. Hikichi and N. Mizuno, *Inorg. Chem.*, 2006, **45**, 9448; (f) A. Lesbani, R. Kawamoto, S. Uchida and N. Mizuno, *Inorg. Chem.*, 2008, **47**, 3349; (g) R. Atencio, A. Briceño and X. Galindo, *Chem. Commun.*, 2005, 637; (h) H. An, D. Xiao, E. Wang, Y. Li and L. Xu, *New J. Chem.*, 2005, **29**, 667; (i) H. An, D. Xiao, E. Wang, Y. Li, X. Wang and L. Xu, *Eur. J. Inorg. Chem.*, 2005, 854.

Chapter 5 Conclusions and perspectives

In conclusion, we have studied the assembly, crystallography and functions of Waugh, Keggin and Anderson POMs-based materials. The prime results are as follows:

(1) By using transition-metal fragment as a linker, a sandwich tetracobalt(II) substituted tungstosilicate $K_{10}[Co_4(H_2O)_2(B\text{-}\alpha\text{-}SiW_9O_{34}H)_2]\cdot 21H_2O$ has been synthesized. This compound offers ideal structural supports for the study of the interactions between paramagnetic metal atoms as well as between delocalized electrons and paramagnetic metal atoms.

(2) By introducing lanthanide fragments, a series organic-inorganic hybrids based on Keggin tungstophosphates ($[Ln(NMP)_6(PW_{12}O_{40})_n]$ (NMP = *N*-methyl-2-pyrrolidone) (Ln = Pr, Eu, Gd) and $[Ln_2(NMP)_{12}(PW_{12}O_{40})][PW_{12}O_{40}]$ (Ln = Gd, Er)) have been synthesized. The compound $[Eu(NMP)_6(PW_{12}O_{40})_n]$ can be used as a Zn^{II}-selective sensor. The compound $[Gd_2(NMP)_{12}(PW_{12}O_{40})][PW_{12}O_{40}]$ has interesting photochromic properties and undergoes an unusual photo-induced single-crystal-to-single-crystal (SCSC) phase transformation.

(3) By using the Anderson-type anion and the lanthanide cation, we have constructed the simple but highly hydrophilic polyoxometalate $[Tm_2(H_2O)_{14}CrMo_6O_{24}H_6][CrMo_6O_{24}H_6]\cdot 16H_2O$ and reported its temperature-dependent SCSC phase transformation that occurs at surprisingly low temperature (< 113 K). Furthermore, this compound can undergo a few desorption and adsorption cycles.

The future work will base on the three kinds of POMs blocks to extend our research. The detailed plan is as follows:

1. Investigation of adsorption properties of $K_{10}[Co_4(H_2O)_2(B\text{-}\alpha\text{-}SiW_9O_{34}H)_2]\cdot 21H_2O$

Polyoxometalates, which are nano-sized metal-oxide macroanions and show unique redox or acidic properties, can create molecular-sized spaces within them or in the solid state with the combination of appropriate cations [1–3]. For example, N. Mizuno's group have well reported a series of compounds $Na_2[Cr_3O(OOCH)_6(H_2O)_3][\alpha\text{-}PW_{12}O_{40}]\cdot 16H_2O$ [**1a**], $K_3[Cr_3O(OOCH)_6(H_2O)_3][\alpha\text{-}SiW_{12}O_{40}]\cdot 16H_2O$ [**2a**], $Rb_4[Cr_3O(OOCH)_6(H_2O)_3][\alpha\text{-}BW_{12}O_{40}]\cdot 16H_2O$ [**3a**], and $Cs_5[Cr_3O(OOCH)_6(H_2O)_3][\alpha\text{-}CoW_{12}O_{40}]\cdot 7.5H_2O$ [**4a**] (Fig. 1) [1–3]. The compound **1b** reversibly sorbed various kinds of polar (hydrophilic) organic molecules such as alcohols, nitriles, and esters as well as water. Neither hydrophobic dichloromethane and dichloroethane nor molecules without or with small polarity such as nitrogen monoxide, dinitrogen, and methane were sorbed despite the small sizes. The compound **2b** sorbed water, methanol, ethanol, acetonitrile, and methyl formate. The compound **3b** sorbed water and methanol, and **4b** sorbed only water. The adsorption properties of **1b**–**4b** depended on not only the molecular sizes but also the dipole moments.

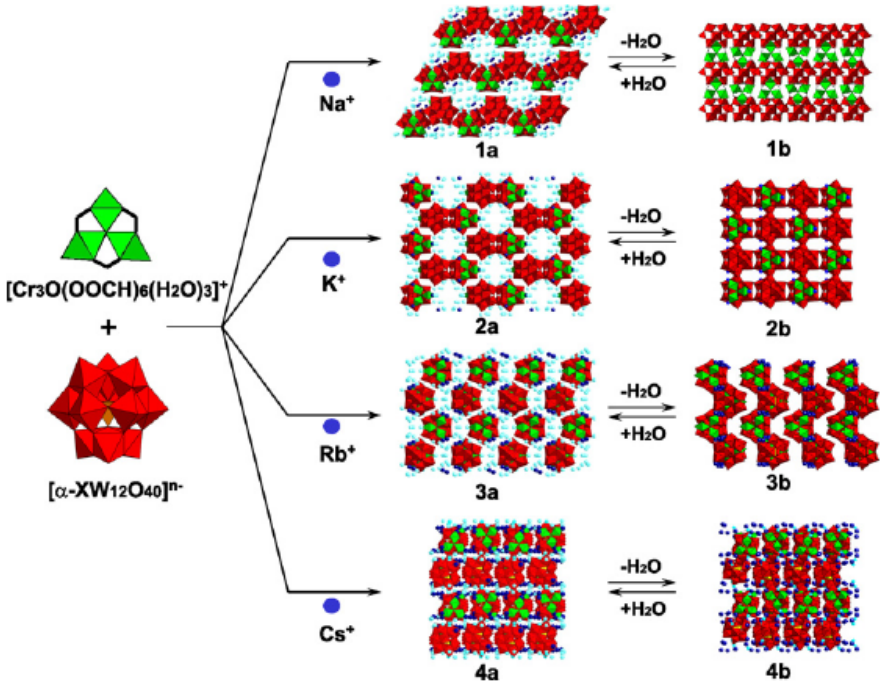

Fig. 1 A series of POMs-based hydrophilic compounds.

On the other hand, as the largest subclass of transitional metal substituted polyoxometalates (TMSPs), sandwich-type compounds have received considerable interest for their magnetism [4]. However, these compounds have received less attention for their adsorption properties [5]. The sandwich-type compound $K_{10}[Co_4(H_2O)_2(B\text{-}\alpha\text{-}SiW_9O_{34}H)_2]\cdot 21H_2O$ (**1a**) has been successfully synthesized in our preliminary work [6]. After removal of water molecules, the compound displays a 3D porous framework (Fig. 2). It is very interesting to investigate its adsorption properties.

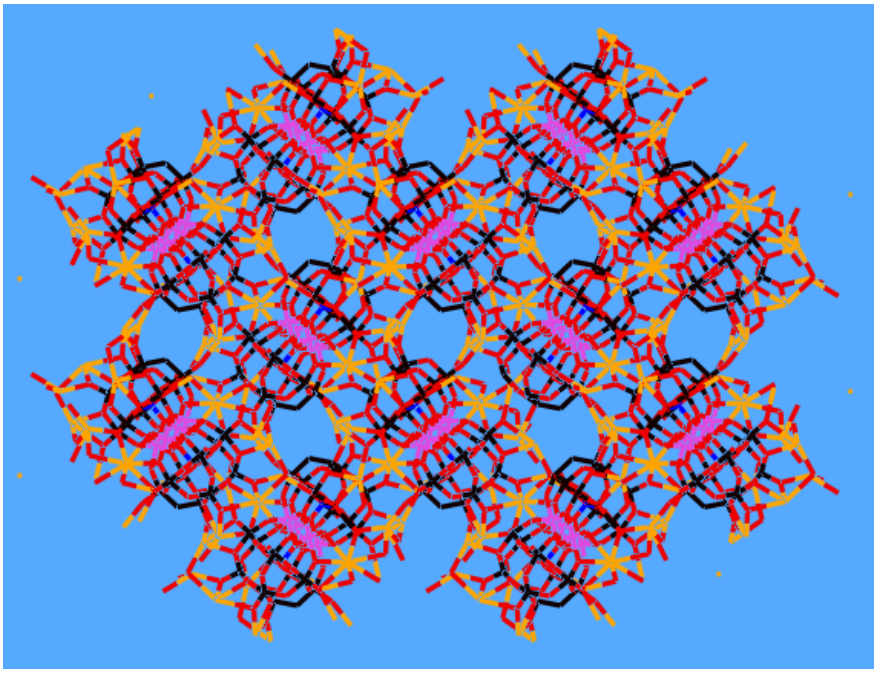

Fig. 2 3D porous framework of $K_{10}[Co_4(B\text{-}\alpha\text{-}SiW_9O_{34}H)_2]$ running to the *a* axis. The color code is as follows: potassium (yellow), cobalt (purple), tungsten (black), silicon (blue), and oxygen (red).

2. Synthesis and properties of derivatives of $K_{10}[Co_4(H_2O)_2(B\text{-}\alpha\text{-}SiW_9O_{34}H)_2]\cdot 21H_2O$

The preparation of organic-inorganic hybrid sandwich POMs have been becoming a research focus in POMs chemistry [7]. For example, in 2006, Niu et al. firstly reported a 1D chainlike architecture built by tetra-Cu sandwiched germanotungstates and $[Cu(en)2]^{2+}$ cationsv [7a]. In 2007, Yang et al. reported a family of novel 2-D tetra-metal sandwiched polyoxotungstates [7b, 7c]. In 2008, Niu et al. reported a novel sandwich germanotungstates

decorated by transition-metal complexes $(C_6N_2H_{18})_3H_2[\{Co(2,2'\text{-bpy})\}_2Co_4(H_2O)_2(\alpha\text{-}GeW_9O_{34})_2]\cdot 4H_2O$ (Fig. 3) [7e]. Covalent grafting of organic functions allows to tune the redox, solubility and acid–base properties, to facilitate their implementation in extended structures and functional devices [8]. Herein, we will further synthesize the derivatives of $K_{10}[Co_4(H_2O)_2(B\text{-}\alpha\text{-}SiW_9O_{34}H)_2]\cdot 21H_2O$ and compare their properties (magnetism and adsorption properties) with the matrix compound $K_{10}[Co_4(H_2O)_2(B\text{-}\alpha\text{-}SiW_9O_{34}H)_2]\cdot 21H_2O$.

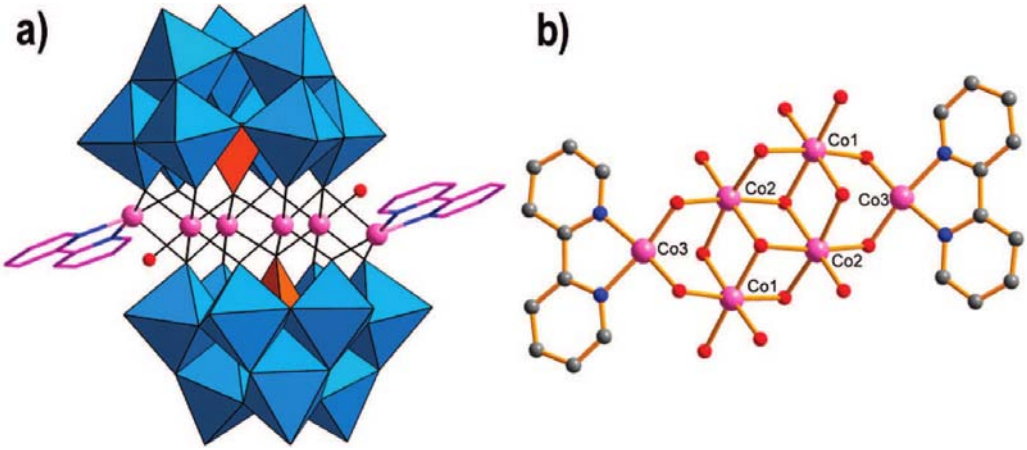

Fig. 3 Polyhedral/ball-and-stick representation of polyoxoanion (a) and the central belt of polyoxoanion (b) in $(C_6N_2H_{18})_3H_2[\{Co(2,2'\text{-bpy})\}_2Co_4(H_2O)_2(\alpha\text{-}GeW_9O_{34})_2]\cdot 4H_2O$. The WO_6 octahedra and GeO_4 tetrahedra are shown in blue and orange, respectively, and the balls represent Co (pink), C (gray), N (blue), and O (red).

3. Photomagnetic properties of $[Gd_2(NMP)_{12}(PW_{12}O_{40})][PW_{12}O_{40}]$

Molecular systems undergoing a reversible and controlled change of their physical properties following a change in an external parameter offer an appealing perspective for the realization of molecular-scale electronic devices [9, 10]. In particular, molecules showing photochromism are of potential interest as materials for optical data storage [11]. A dramatic extension of the perspectives of photochromism was given by the development of molecular magnetism [12, 13], which lead to the discovery that the switching of the magnetic properties

of a molecule and long-range magnetic-order effects can be induced by photo-excitation [14, 15].

We have reported five compounds based on Keggin tungstophosphates ($[Ln(NMP)_6(PW_{12}O_{40})_n]$ (Ln = Pr, Eu, Gd) and $[Ln_2(NMP)_{12}(PW_{12}O_{40})][PW_{12}O_{40}]$ (Ln = Gd, Er)) [16, 17]. These compounds are all photochromic. Especially, for $[Gd_2(NMP)_{12}(PW_{12}O_{40})][PW_{12}O_{40}]$, a reversible photopolymerization (SCSC transformation) from 0-D to 1-D interestingly occurred. Since there is not only SCSC transformation but also deoxidized W^V atoms under irradiation with sunlight, it is highly interesting to investigate the photomagnetism of $[Gd_2(NMP)_{12}(PW_{12}O_{40})][PW_{12}O_{40}]$.

Before and after irradiation under sunlight for 5 h, the magnetic properties are changeful, two curves for experimental data plotted as $\chi_M T$ versus T shown in Fig. 4a respectively. The black curve represents the magnetism of the original colorless compound with the $\chi_M T$ at room temperature, 15.6 cm^3 K mol^{-1}, which is slightly smaller than the spin-only value of 15.75 cm^3 K mol^{-1} for the magnetically isolated two-spin Gd^{III} system. Under sunlight for 5 h, one of W^{VI} atoms of each polyoxoanion is reduced into W^V with the SCSC transformation from zero-D to 1-D, leading to the appearance of the red magnetic curve with the $\chi_M T$ at room temperature, 16.4 cm^3 K mol^{-1}, in agreement with that of two isolated Gd^{III}-W^V units. The photomagnetic effect may be observed as well in the magnetization curves, performed at 2 K and shown in Fig. 4b. Before irradiation, the data correspond to an isolated spin S = 7/2 (Gd^{III} ions). After irradiation, the magnetization data shows a value at 8 at 50 kOe. In addition, the EPR spectra before and after irradiation are also measured (Fig. 4c), which can qualitatively indicates the photomagnetic effect.

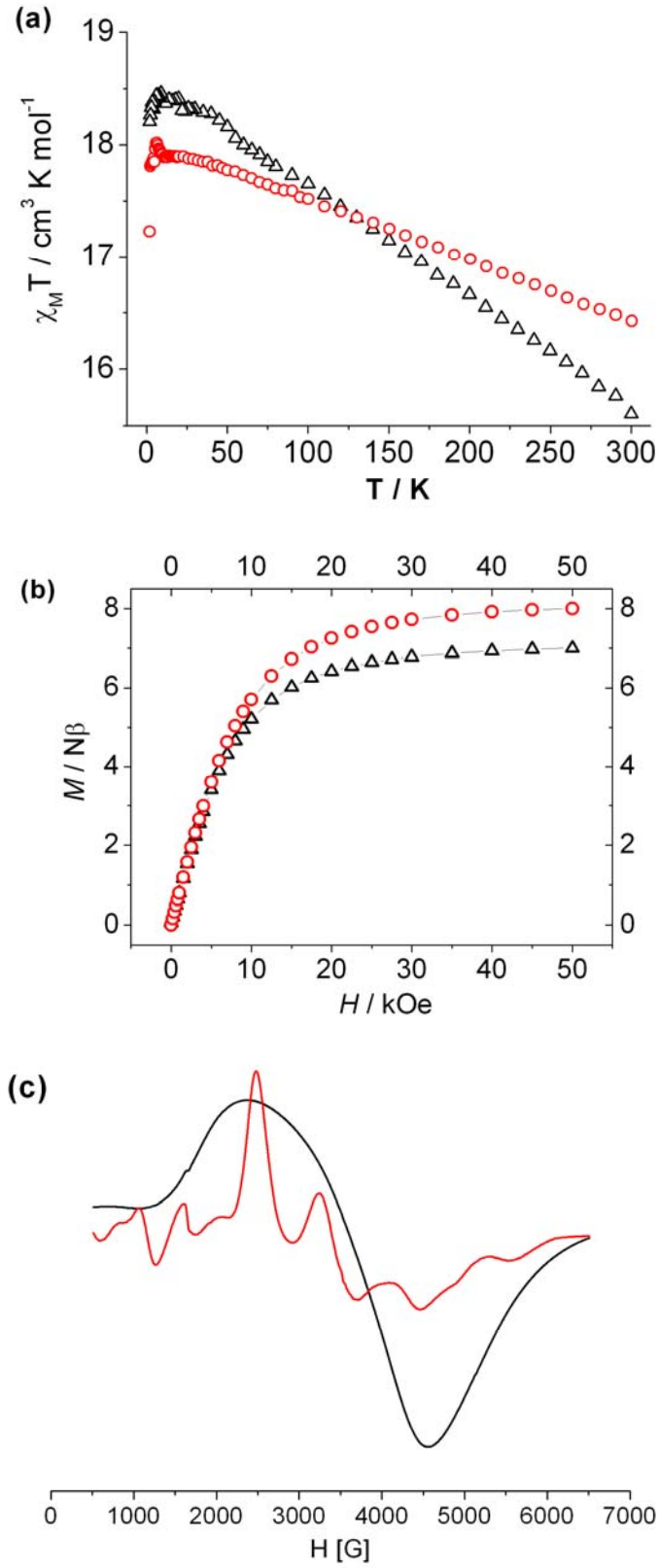

Fig. 4 (a) Photomagnetic plots of $\chi_M T$ versus T ; (b) Field dependence of the magnetization M at 2 K; (c) EPR spectra before (Δ, black) and after (O, red) irradiation for 5 h.

Different from the other coordination complexes showing photo-induced magnetic properties [14, 15], to the best of our knowledge, the photomagnetic compound is the first example based on polyoxometalates, which provides a new way to design photomagnetic switching materials. By the introduction of different polyoxoanions and paramagnetic metal ions, more novel photomagnetic compounds with various extended-structures based on polyoxometalats would be obtained.

4. Design and synthesis of photochromic materials based on Keggin tungstophosphates and azobenzene

Our preliminary work indicated that materials based on Keggin tungstophosphates displayed interesting photochromic properties, and a photo-induced SCSC phase transformation unexpectedly occurred. In order to extend our research, we will explore another system based on Keggin tungstophosphates and azobenzene.

As is well-known, azobenzene and many of its derivatives are characterized by reversible transformations from the generally more stable *trans* form to the less stable *cis* form upon irradiation with UV or visible light to yield a photo-stationary composition that is wavelength and temperature dependent (Scheme 1) [18]. On the other hand, azobenzene and its derivatives can be a donor to provide electrons, which can be used for the design of POMs-based photochromic materials.

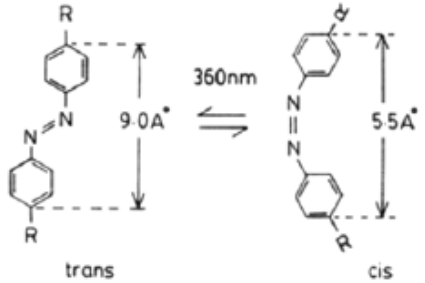

Scheme 1

Herein, we construct the system based on Keggin tungstophosphates and azobenzene, which would be a good candidate for the studies of photochromism and photo-induced SCSC phase transformations.

5. Functional compounds built on Anderson POMs

We have communicated the simple but highly hydrophilic compound $[Tm_2(H_2O)_{14}CrMo_6O_{24}H_6][CrMo_6O_{24}H_6]\cdot 16\ H_2O$ by using the Anderson-type anion $[CrMo_6O_{24}H_6]^{3-}$ and the lanthanide cation Tm^{3+} [19]. Here, by introduce different lanthanide cations (e.g. Eu^{3+}, Gd^{3+}, Tb^{3+}), a series of compounds $\{[Ln(H_2O)_7[CrMo_6O_{24}H_6]\cdot 4H_2O\}_n$ (Ln = Eu^{3+}, Gd^{3+}, Tb^{3+}) can be successfully synthesized. These compounds consist of 1D infinite zigzag chains built from alternate polyoxoanions $[[CrMo_6O_{24}H_6]^{3-}$ and $[Ln(H_2O)_7]^{3+}$ subunits (Fig. 5) (The summary of crystallographic data is given in Table 1). We choose $\{[Eu(H_2O)_7[CrMo_6O_{24}H_6]\cdot 4H_2O\}_n$ to represent the detailed structure. As shown in Fig. 5a, the adjacent Eu···Eu distances are 10.961 Å. The coordination polyhedron of Eu^{3+} can be represented as a distorted, tricapped trigonal prism (Fig. 5b). The Eu−O bond lengths are within the range from 2.366 to 2.583 Å (mean value 2.447 Å). The torsion angle between the top plane and the bottom plane is 7.52 °. The Eu^{3+} and Cr^{3+} are linked by O_c−Mo−O_a with the separation 7.153 Å. The angle of Eu···Cr···Eu is 101.07 °.

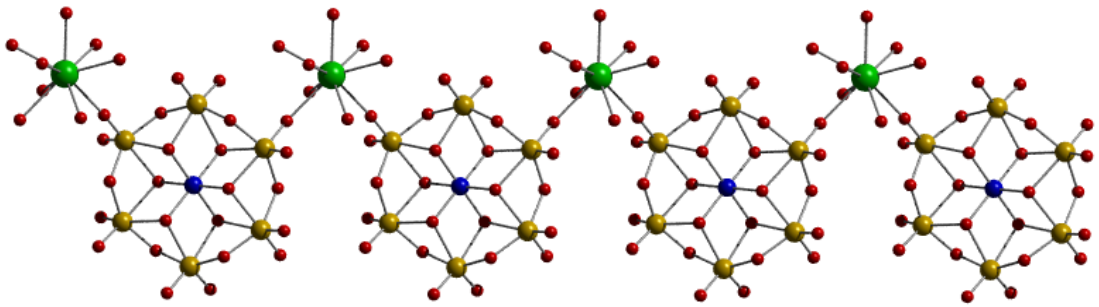

(a)

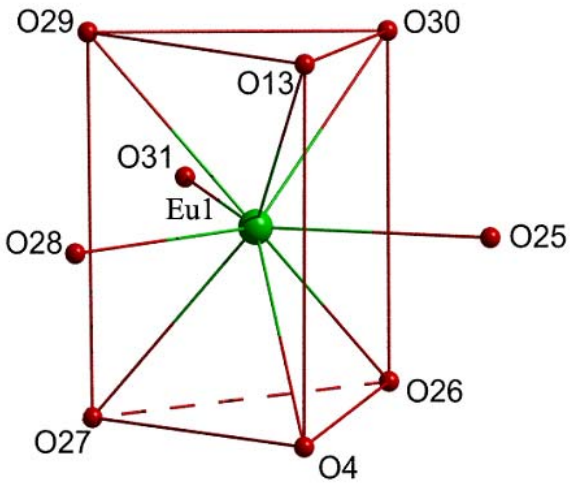

(b)

Fig. 5 (a) Ball-stick view of the 1D assembly chain in $\{[Eu(H_2O)_7[CrMo_6O_{24}H_6]\cdot 4H_2O\}_n$; (b) coordination polyhedron around Eu^{3+}. The color code is as follows: Eu (green), O (red), Cr (blue), Mo (yellow).

Variable-temperature (2−300 K) magnetic susceptibility data at a magnetic field strength of 2 kG were collected for $\{[Gd(H_2O)_7[CrMo_6O_{24}H_6]\cdot 4H_2O\}_n$ (Fig. 6). The magnetic data can be analyzed by the following approximate treatment equations:

$$\chi = \frac{N\beta^2}{3kT}\left[g^2 + g^2\frac{1+\mu}{1-\mu} + \theta^2\frac{1-\mu}{1+\mu}\right]$$

$$g = (g_A^e + g_B^e)/2$$

$$\theta = (g_A^e - g_B^e)/2$$

$$\mu = Coth\,(J^e/kT) - (kT/J^e)$$

$$g_A^e = g_A[S_A(S_A+1)]^{1/2}$$

$$g_B^e = g_B[S_B(S_B+1)]^{1/2}$$

$$J^e = J[S_AS_B(S_A+1)(S_B+1)]^{1/2}$$

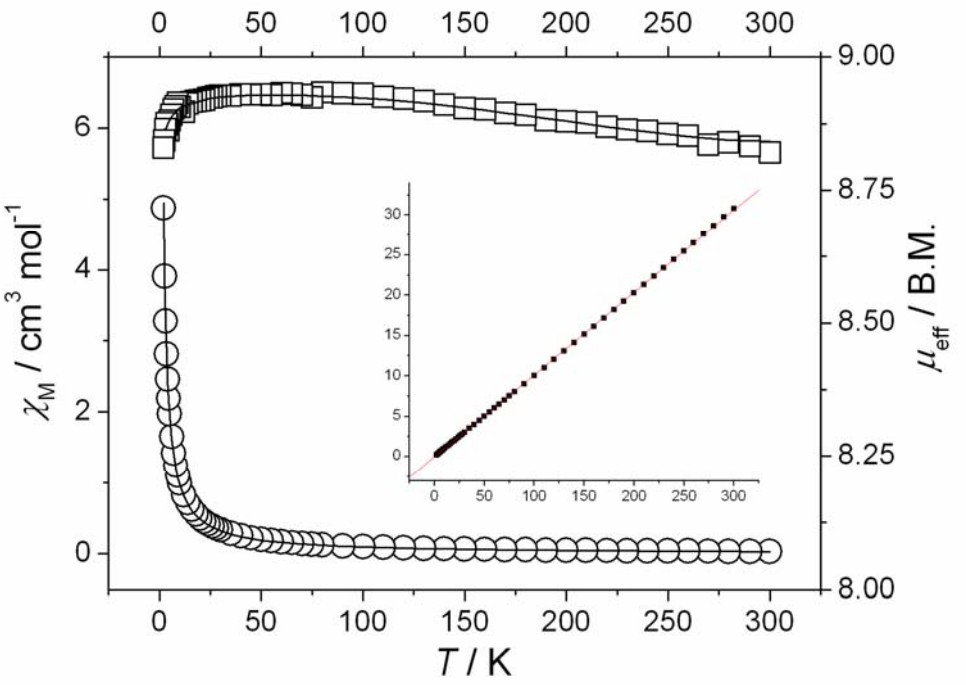

Fig. 6 Plots of $\chi_M T$ and χ_M versus T for $\{[Gd(H_2O)_7[CrMo_6O_{24}H_6]\cdot 4H_2O\}_n$.

The emission spectrum of $\{[Tb(H_2O)_7[CrMo_6O_{24}H_6]\cdot 4H_2O\}_n$ (Fig. 7) at room temperature in the solid state excited at 285 nm exhibited the characteristic transition of the Tb^{3+} ion: $^5D_4 \rightarrow {}^7F_J$ ($J = 6, 5$).

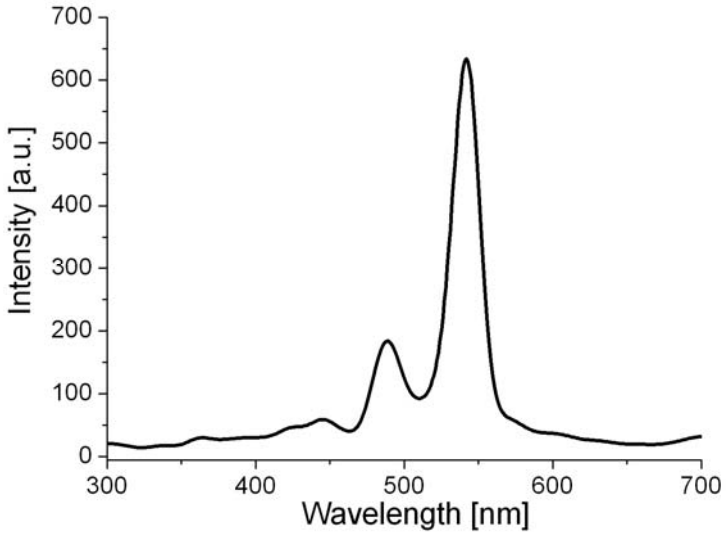

Fig. 7 Solid-state emission spectra of $\{[Tb(H_2O)_7[CrMo_6O_{24}H_6]\cdot 4H_2O\}_n$ at room temperature (excited at 285 nm).

The further work will study the structural changes with lanthanide contraction, and detailedly discuss magnetic, luminescent properties. Moreover, the adsorption properties and temperature-dependent SCSC phase transformation will be also explored.

Table 1 Crystal data and structure refinement of $\{[Ln(H_2O)_7[CrMo_6O_{24}H_6]\cdot 4H_2O\}_n$ (Ln = Eu^{3+}, Gd^{3+}, Tb^{3+}).

Empirical formula	$H_{28}CrMo_6O_{35}Eu$	$H_{28}CrMo_6O_{35}Gd$	$H_{28}CrMo_6O_{35}Tb$
Formula weight	1367.82	1373.11	1368.74
Temperature	294(2) K	294(2) K	294(2) K
Wavelength	0.71073 Å	0.71073 Å	0.71073 Å
Monochromator	Graphite	Graphite	Graphite
Crystal System	Orthorhombic	Orthorhombic	Orthorhombic
Space group	*P*ca2(1)	*P*ca2(1)	*P*ca2(1)
Unit cell dimensions	a = 11.8308(13) Å α = 90° b = 10.9614(13) Å β = 90° c = 22.421(3) Å γ = 90°	a = 11.833(2) Å α = 90° b = 10.959(2) Å β = 90° c = 22.399(5) Å γ = 90°	a = 11.8008(11) Å α = 90° b = 10.9265(10) Å β = 90° c = 22.312(2) Å γ = 90°
Volume	2907.6(6) $Å^3$	2904.6(10) $Å^3$	2877.0(5) $Å^3$
Z	4	4	4
Density (calculated)	3.125 Mg m^{-3}	3.140 Mg m^{-3}	3.160 Mg m^{-3}
Absorption coefficient	5.109 mm^{-1}	5.238 mm^{-1}	5.441 mm^{-1}
F (000)	2588	2592	2572
Crystal size	0.20 × 0.16 × 0.12 mm	0.10 × 0.09 × 0.06 mm	0.28 × 0.26 × 0.22 mm
θ range for data collection	1.82 to 26.41°	1.82 to 27.87°	1.83 to 26.39°
Limiting indices	$-14 \le h \le 14$, $-12 \le k \le 13$, $-28 \le l \le 18$	$-14 \le h \le 15$, $-14 \le k \le 14$, $-29 \le l \le 20$	$-14 \le h \le 11$, $-13 \le k \le 13$, $-27 \le l \le 20$
Reflections collected/unique	15688 / 4696 [R_{int} = 0.0565]	25877 / 6255 [R_{int} = 0.0374]	15619 / 5151 [R_{int} = 0.0346]
Absorption correction	Semi-empirical from equivalents	Semi-empirical from equivalents	Semi-empirical from equivalents
Refinement method	Full-matrix least-squares on F^2	Full-matrix least-squares on F^2	Full-matrix least-squares on F^2
Data/restraints/parameters	4696 / 7 / 389	6255 / 25 / 395	5151 / 25 / 390
Goodness-of-fit on F^2	1.073	1.013	0.962
Final R indices [$I>2\sigma(I)$]	R_1 = 0.0335, wR_2 = 0.0668	R_1 = 0.0254, wR_2 = 0.0505	R_1 = 0.0246, wR_2 = 0.0585
R indices (all data)	R_1 = 0.0487, wR_2 = 0.0725	R_1 = 0.0298, wR_2 = 0.0521	R_1 = 0.0281, wR_2 = 0.0601

References

[1] S. Uchida, M. Hashimoto and N. Mizuno, *Angew. Chem., Int. Ed.*, 2002, **41**, 2814.

[2] S. Uchida and N. Mizuno, *J. Am. Chem. Soc.*, 2004, **126**, 1602.

[3] S. Uchida, R. Kawamoto and N. Mizuno, *Inorg. Chem.*, 2006, *45*, 5136.

[4] (a) U. Kortz, S. Nellutla, A. C. Stowe, N. S. Dalal, J. van Tol and B. S. Bassil, *Inorg. Chem.*, 2004, **43**, 144; (b) S. Nellutla, J. van Tol, N. S. Dalal, L. -H. Bi, U. Kortz, B. Keita, L. Nadjo, G. A. Khitrov and A. G. Marshall, *Inorg. Chem.*, 2005, **44**, 9795. (c) U. Kortz, S. Isber, M. H. Dickman, D. Ravot, *Inorg. Chem.*, 2000, **39**, 2915; (d) C. J. Gómez-García, E. Coronado, P. Gómez-Romero and N. Casañ-Pastor, *Inorg. Chem.*, 1993, **32**, 3378.

[5] (a)M. Hölscher, U. Englert, B. Zibrowius and W. F. Hölderich, *Angew. Chem., Int. Ed. Engl.*, 1994, **33**, 2491; (b) D. Hagrman, P. J. Hagrman and J. Zubieta, *Angew. Chem., Int. Ed.*, 1999, **38**, 3165; (c) J. H. Son, H. Choi and Y. U. Kwon, *J. Am. Chem. Soc.*, 2000, **122**, 7432; (d) C. Du Peloux, A. Dolbecq, P. Mialane, J. Marrot, E. Rivière, F. Sécheresse, Angew. Chem., Int. Ed., 2001, **40**, 2455; (e) M. V. Vasylyev, R. Neumann, *J. Am. Chem. Soc.*, 2004, **126**, 884; Y. Ishii, Y. Takenaka and K. Konishi, Angew. Chem., Int. Ed., 2004, **43**, 2702; (f) S. S. Mal, U. Kortz, *Angew. Chem., Int. Ed.*, 2005, **44**, 3777; (g) H. A. An, E. B. Wang, D. R. Xiao, Y. G. Li, Z. M. Su and L. Xu, *Angew. Chem., Int. Ed.*, 2006, **45**, 904.

[6] L. -Z. Zhang, W. Gu, X. Liu, Z. L. Dong, Y. -S. Yang, B. Li and D. -Z. Liao, *Inorg.Chem. Commun.*, 2007**, 10**, 1378.

[7] (a) J. P. Wang, X. D. Du and J. Y Niu, *Chem. Lett.*, 2006, **35**, 1408; (b) S. T. Zheng, M. H. Wang and G. Y. Yang, *Chem. Asian J.*, 2007, **2**, 1380; (c) J. W. Zhao, B. Li, S. T. Zheng and G. Y. Yang, *Cryst. Growth Des.*, 2007, **7**, 2658; (d) Z. Zhang, J. Liu, E. Wang, C. Qin, Y. Li, Y. Qi and X. Wang, *Dalton Trans.*, 2008, 463; (e) J. Wang, P. Ma, Y. Shen and J. Niu, *Cryst. Growth Des.*, 2008, **8**, 3130.

[8] A. Proust, René Thouvenot and P. Gouzerh, *Chem. Commun.*, 2008, 1837

[9] B. L. Feringa, Molecular Switches, Wiley-VCH, Weinheim, Germany, 2001.

[10] A. P. de Silva and N. D. McClenaghan, *Eur. −J. Chem.*, 2004, **10**, 574.

[11] Special issue “Photochromism: Memories and Switches” M. Irie (Guest Ed.), *Chem. Rev.*, 2000, **100**, 1683.

[12] O. Khan, Molecular Magnetism, Wiley-VCH, Weinheim, 1993.

[13] Magnetism: molecules to materials (Eds.: J. S. Miller and M. Drillon), Wiley-VCH, Weinheim, 2001.

[14] P. Gütlich, Y. Garcia and T. Woike, *Coord. Chem. Rev.*, 2001, **219–221**, 839.

[15] O. Sato, *Acc. Chem. Res.*, 2003, **36**, 692.

[16] L. -Z. Zhang, W. Gu, X. Liu, Z. L. Dong and B. Li, *CrystEngComm*, 2008, **10**, 652.

[17] L. -Z. Zhang, W. Gu, Z. L. Dong, X. Liu, B. Li and M. L. Liu, *J. Solid State Chem.*, 2009, **182**, 1040.

[18] G. S. Kumar and D. C. Neckers, *Chem.Rev.*, 1989, **89**, 1915.

[19] L. -Z. Zhang, W. Gu, Z. L. Dong, X. Liu and B. Li, *CrystEngComm*, 2008, **10**, 1318.

Publications

[1] L.-Z. Zhang, W. Gu, Z.L. Dong, X. Liu, B. Li, M.L. Liu, Syntheses, structures and properties of a series of photochromic hybrids based on Keggin tungstophosphates, *J. Solid State Chem.*, **2009**, *182*, 1040.

[2] L.-Z. Zhang, W. Gu, Z.L. Dong, X. Liu, B. Li, Phase transformation of a rare-earth Anderson polyoxometalate at low temperature, *CrystEngComm*, **2008**, *10*, 1318.

[3] L.-Z. Zhang, W. Gu, X. Liu, Z.L. Dong, B. Li, Solid-state photopolymerization of a photochromic hybrid based on Keggin tungstophosphates, *CrystEngComm*, **2008**, *10*, 652.

[4] L.-Z. Zhang, W. Gu, X. Liu, Z.L. Dong, Y.-S. Yang, B. Li, D.-Z. Liao, $K_{10}[Co_4(H_2O)_2(B\text{-}\alpha\text{-}SiW_9O_{34}H)_2]\cdot 21H_2O$: A sandwich polyoxometalate based on the magnetically interesting element cobalt, *Inorg. Chem. Commun.*, **2007,** *10*, 1378.